UNITED STATES DEPARTMENT OF THE INTERIOR

GEOLOGICAL SURVEY

VITRINITE REFLECTANCE AND ESTIMATES OF PALEOTEMPERATURE FOR FRANCISCAN TERRANES OF COASTAL NORTHERN CALIFORNIA: 40°00'N to 40°35'N

Michael B. Underwood[1,2] and Robert H. Strong[2]

Open-File Report 86-258

This report was prepared under a grant from the U.S. Geological Survey and has not been reviewed for conformity with USGS editorial standards and stratigraphic nomenclature. Opinions and conclusions expressed herein do not necessarily represent those of the USGS. Any use of trade names is for descriptive purposes only and does not imply endorsement by the USGS.

[1]U.S. Geological Survey
Branch of Pacific-Marine Geology
Menlo Park, CA

[2]Department of Geology
University of Missouri
Columbia, MO

1986

PREFACE

This report summarizes trends in thermal maturity for strata of the Franciscan Complex in coastal northern California. The study area is located between latitudes 40°00'N and 40°35'N. A companion report by Underwood and O'Leary (1985) describes relationships immediately to the south. All data were derived from measurements of vitrinite reflectance using surface samples.

ACKNOWLEDGMENTS

All analyses were complete at the University of Missouri, Columbia. Laboratory assistance was provided by Chris Gillett, Pad Quinn, and Jack O'Leary. We thank David Houseknecht for valuable advise regarding organic petrography. Some Franciscan samples were collected by Bob McLaughlin, Steve Ellen, and M. Clark Blake. Funding was provided by the U.S. Department of Energy and administered to the University of Missouri through USGS Purchase Order No. 110178. A review by Keith Kvenvolden improved the clarity of the report.

TABLE OF CONTENTS

LIST OF FIGURES

LIST OF TABLES

INTRODUCTION

The Franciscan Complex in northern California is subdivided into several tectonostratigraphic units based on structural style, general lithologic content, depositional age, metamorphic grade, and sandstone petrography. Boundaries between terranes are either diffuse structural transitions or more clearly-defined faults. Blueschist-facies metamorphism is common, but the metamorphic grade decreases to zeolite facies in the western portion of the complex (Blake and Jones, 1981). Ages of fossils also follow a westward decreasing trend and range from Late Jurassic to Miocene (Blake and Jones, 1974; Evitt and Pierce, 1975; Bachman, 1978; McLaughlin et al., 1982).

Most workers believe the Franciscan Complex is a product of subduction tectonics. In the simplest view, Franciscan strata were accreted directly to the western margin of North America as a consequence of late Mesozoic to middle Tertiary subduction (e.g., Bachman, 1982; Ernst, 1983,1984). Other workers have taken a more mobilistic approach, however, and suggest that translational motions were at least as important as simple orthogonal convergence (e.g., Blake and Jones, 1981; McLaughlin et al., 1982).

The details of Franciscan structural and burial history remain poorly understood, and the primary intent of our study is to focus on spatial trends in thermal maturity and their implications for burial history. Past studies of Franciscan burial history have concentrated on metamorphic mineral assemblages (e.g., Blake et al., 1967; Ernst, 1971; Ernst et al, 1970; Cloos, 1983). Although temperature-pressure regimes have been determined for minerals such as laumontite, pumpellyite, and lawsonite, these mineral transformations occur over a broad range of conditions and are subject to complex interactions of physical and chemical factors. For example, lawsonite is stable at pressures of 4-8 K bars (15-30 km depth of burial) and temperatures of 150°-400°C (see Turner, 1981, for summary). At lower temperatures and pressures, the stability ranges of zeolite-grade minerals can be affected by even more variables (Castano and Sparks, 1974; Ghent, 1979).

Studies of organic metamorphism within the Franciscan are limited in number. Bachman (1978) used thermal alteration index to estimate a depth of burial of roughly 4700 meters near Ft. Bragg. Bostick (1974) estimated temperatures ranging from 155°-250°C in the Diablo antiform using vitrinite reflectance. Vitrinite-reflectance data also demonstrate that Yager strata in southern Humboldt County were subjected to temperatures of less than 200°C (Underwood, 1985). The technique of vitrinite reflectance represents a powerful tool for studies of orogenic history because reflectance values span a temperature range from early diagenesis to greenschist-facies metamorphism (i.e., 25°C to at least 400°C; Price and Barker, 1985). Moreover, vitrinite records only the peak temperature to which host rocks were exposed.

The purpose of our study is to document relative levels of thermal maturity within the Franciscan terranes using the technique of vitrinite reflectance (Ro). All samples were obtained from surface exposures. Three specific goals have been identified: (1) to determine the overall magnitude of thermal maturity for each Franciscan terrane, (2) to identify surface anomalies and/or gradients in Ro values, especially as related to terrane boundaries, and (3) to integrate thermal-maturity data with existing structural and stratigraphic information in order to reconstruct the history of burial. This report provides a brief summary of our findings, together with descriptions of technique and a complete tabulation of data.

STUDY AREA

The study area is located in the northern Coast Ranges of California between latitudes 40°00'N and 40°35'N (Fig. 1). The first detailed geologic investigation within this region was conducted by Ogle (1953). Subsequent workers included Irwin (1960), Evitt and Pierce (1975), Herd (1978), Beutner and others (1980), McLaughlin and others (1982), Underwood (1982, 1984, 1985), and Bachman and others (1984). The four principal Franciscan terranes of the region are the Central belt (upper Mesozoic), the Coastal belt (Upper Cretaceous to Oligocene), the Yager complex (Paleocene to Oligocene), and the King Range (Eocene to Miocene) (Fig. 2). The Franciscan rocks are unconformably overlain by the Wildcat Group (Neogene to Quaternary).

The boundary between folded turbidites of the Yager complex and older melange of the Central Belt is a prominent thrust, originally named the Coastal Belt thrust (Jones et al., 1978). This fault (Fig. 2) has been given other names, including the Garberville thrust (Underwood, 1982) and the Eel River fault (Bachman et al., 1984). Recent maps segregate Yager strata from the Coastal belt on a regional scale (Bachman et al., 1984; Underwood, 1985), such that Yager beds geographically separate the "Coastal belt" thrust from its namesake, the Coastal belt. Consequently, we believe the "Eel River fault" is a more appropriate name to apply to this important terrane boundary.

To the west, the Yager complex is separated from the Franciscan Coastal belt by a diffuse structural zone called the Coastal Belt transition (Fig. 2; Underwood, 1983). This boundary is defined by a change in structural style; Coastal belt turbidites display typical melange fabrics (scaly argillite, pinch-and swell, etc.) whereas broadly coeval Yager strata do not exhibit penetrative and pervasive stratal disruption. Even so, the boundary can be located only within about 100 m, even in areas of good outcrop (Underwood, 1984).

The contact between the Coastal Belt and the King Range terrane also is poorly constrained. The King Range is bounded on the north and east by shear zones (Ogle, 1953; McLaughlin et al., 1982), but in essence, these shear zones extend across the entire width of the Coastal belt (Underwood, 1984). Moreover, there is a complicated intercalation of tightly-folded (King Range) and pervasively sheared (Coastal belt) strata near the terrane boundary. Consequently, an exact definition of the boundary is difficult to make (Underwood, 1984).

Several high-angle faults are present in the vicinity of Garberville (Fig. 2). These appear to be normal faults, but some component of strike-slip motion cannot be eliminated (Underwood, 1984). Herd (1978) also identified the Lake Mountain fault as a major zone of strike-slip displacement within the eastern edge of the study area (Fig. 2). The fresh geomorphic expression of the fault implies a Quaternary history of movement; it crosses rather than controls topography, so displacements are probably not large. Strike-slip faulting is also evident in the Bear Harbor and Point Delgada areas (McLaughlin et al., 1982).

TECHNIQUES

The technique of vitrinite reflectance is based upon the empirical observation that reflectance values (Ro) in both coals and shales increase exponentially with burial depth (e.g., Dow, 1977; Bostick et al., 1978). Actual measured reflectance values can be biased by several variables, how-

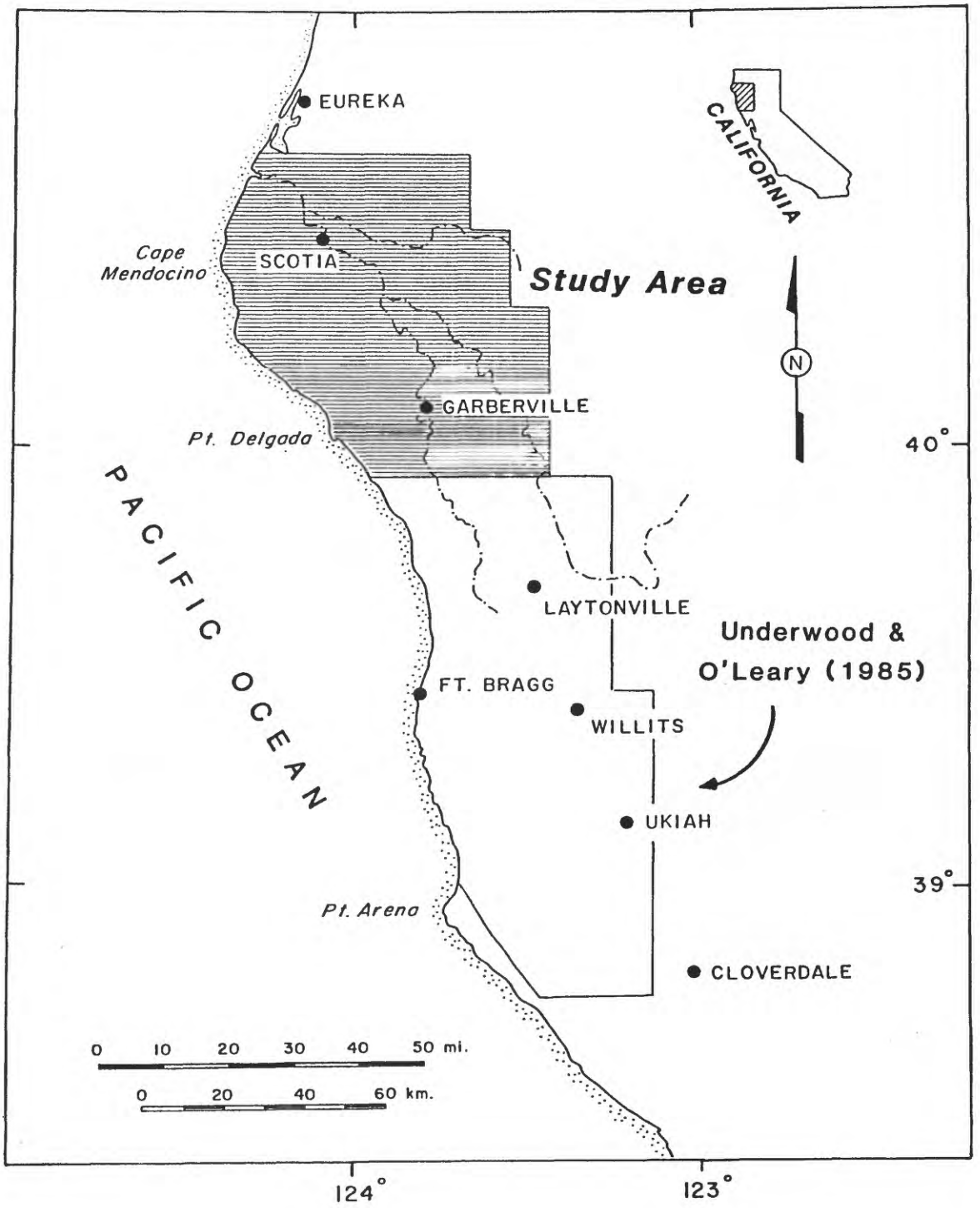

FIGURE 1. Map of coastal northern California showing the location of study area. Region immediately to the south was analyzed for thermal maturity by Underwood and O'Leary (1985).

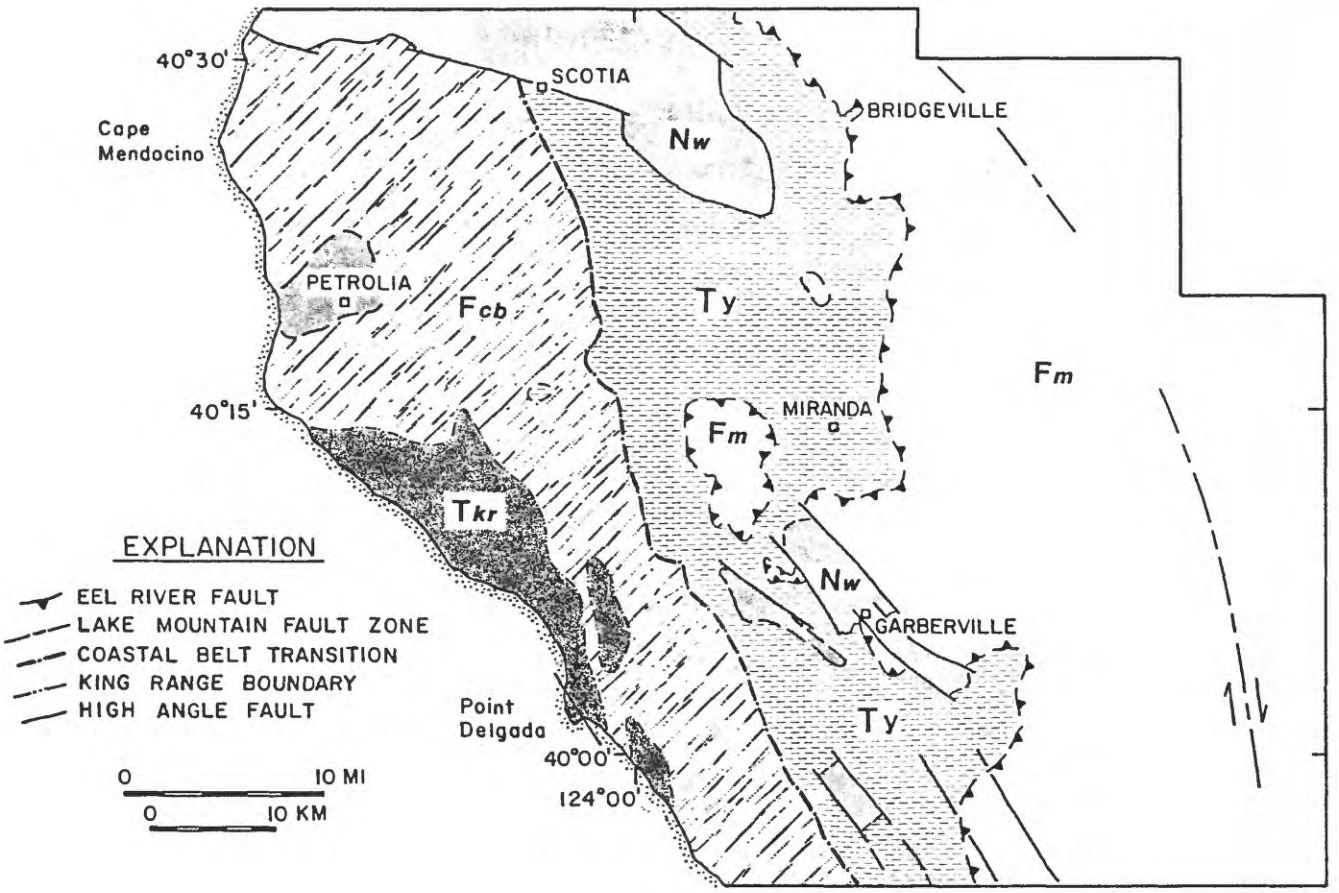

FIGURE 2. Simplified geologic map of the study area showing major structural boundaries and tectonostratigraphic terranes of the Franciscan Complex. Fm = Franciscan Central belt; Ty = Yager complex; Fcb = Franciscan Coastal belt; Tkr = King Range; Nw = Wildcat Group. The geology of this region has been described in detail by Ogle (1953), Irwin (1960), McLaughlin and others (1982), and Underwood (1984, 1985).

ever, and each of these factors is discussed in detail in Appendix A. For example, individual vitrinite particles can be anisotropic in their reflectance, especially at higher levels of maturation (Stach, 1975). This problem is reduced by calculating mean values based upon measurements of numerous individual particles. Mean reflectance (Rm) values are also suppressed by high concentrations of hydrogen-rich exinite and alginite in association with the vitrinite (Hutton and Cook, 1980; Price and Barker, 1985). Furthermore, anaerobic conditions in the environment of deposition tend to depress Ro (Newman and Newman, 1982). Visual assessment of kerogen type and geochemical measurements demonstrate that Type III kerogen is dominant in Franciscan shales (Underwood, 1985; Strong, 1986), so the problem of Ro suppression probably can be ignored.

Because of the resistance of vitrinite to weathering, grains can be recycled from older sedimentary strata. If recycled material is more mature than the present host rock and is left unrecognized, then mean reflectance values become erroneously high. Histograms commonly are used to help identify recycled grains, although selection criteria are somewhat arbitrary (Fig. 3, Appendix A). Computation of an accurate mean (Rm) is also dependent upon proper selection of vitrinite grains for measurements, and two factors tend to influence this selection process in a negative way. First, above Ro = 1.5% convergence begins to occur between the reflectivity of vitrinite and the reflectivity of other organic macerals (Bostick, 1979; Tissot and Welte, 1984). Second, the reflectance of vitrinite itself can be modified by recent weathering at or near the ground surface (Marchioni, 1983). Solutions to these problems are outlined in Appendix A.

A final unresolved problem is related to the relatively low content of total organic matter in many Franciscan samples (Underwood, 1985; unpublished data). Kerogen was extracted and concentrated following the methods outlined in Appendix A. Many samples contain a paucity of vitrinite, however, and some shales are virtually barren. Nevertheless, we were able to obtain statistically reliable data from roughly 87% of the samples originally collected. The mean values (Rm) reported here are based upon measurements of approximately 50 individual particles per sample.

Several techniques have been proposed to model thermal maturation. For example, Hood and others (1975) proposed a time-temperature model based upon the concepts of maximum temperature (T-max) and effective heating time (i.e. the amount of time within 15°C of T-max). Recent studies, however, have challenged the validity of this method, especially the extrapolation of the Hood scale to lower levels of thermal maturation (Suggate, 1982). A second technique, termed the Lopatin method (Waples, 1980), requires a detailed reconstruction of burial depth versus geologic age, usually for a series of stratigraphic horizons. Because there are so many uncertainties related to Franciscan burial history, the reliability of Lopatin reconstructions remains questionable.

Until recently, it was widely accepted that temperature and time were equally important in organic metamorphism (e.g., Bostick, 1979; Wright, 1980). However, other workers contend that Ro equilibration occurs within 10^4 to 10^6 years and that additional time has little or no influence (Suggate, 1982; Barker, 1983; Price, 1983). A third technique, proposed by Price (1983), uses vitrinite reflectance as an absolute paleogeothermometer. Ammosov and others (1975) developed a similar method, and Price (1983) revised the regression line based upon data from fourteen first-cycle sedimentary basins around the

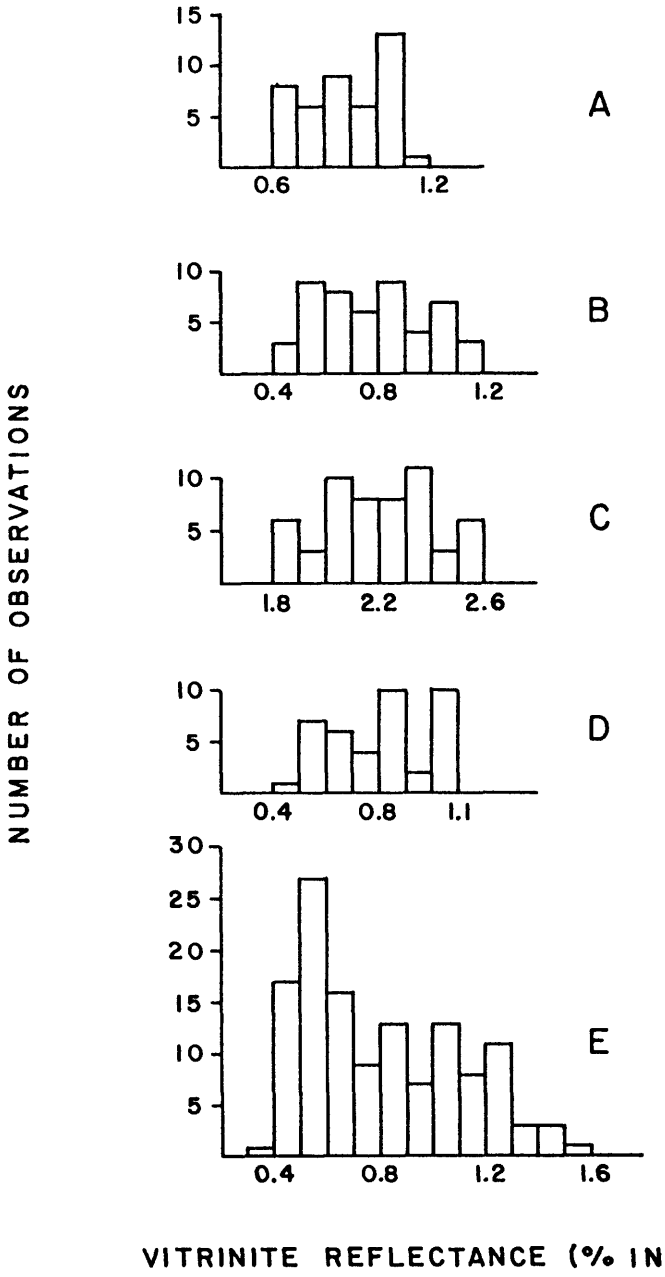

FIGURE 3. Histogram plots of vitrinite-reflectance populations for five individual samples collected in the study area. Multi-modal populations such as these make objective identification of "primary" and "recycled" grains rather difficult. Sample A = EV15-24 (Central belt); Sample B = EV15-30 (Central belt); Sample C = MK-94 (King Range); Sample D = M83-145 (King Range); Sample E = M83-136 (Coastal belt). See Appendix A for additional information regarding statistical treatment of reflectance data.

world. Both paleothermometers are in close agreement below about Ro = 0.90%, but divergence occurs at higher levels of maturity. Price's regression equation is based upon a broad data base, and the correlation coefficient is high ($r = 0.97$); consequently, estimates of paleotemperatures in our study area are based upon the Price method. Interested readers should note that the caption to Price's (1983) Figure 19 was not printed correctly; the regression equation actually applies to Type III kerogen and cannot be used with rocks bearing Type I organic matter (Price, 1985).

It is important to realize that the primary intent of our study is to establish relative differences in thermal maturity rather than absolute values of paleotemperature or burial depth. At the same time, burial depths can be estimated if an appropriate geothermal gradient is determined. Such a choice is problematic. Most measurements of present-day surface heat flow within the study area range from 1.0 to 1.8 HFU (43 to 76 m W/m^2) (Lachenbruch and Sass, 1980). If a thermal conductivity of 6 mcal/cm-s-^oC is used, the present-day geothermal gradient is between 20^oC/km and 30^oC/km, but to assume a constant gradient or thermal conductivity over the past 65 million years probably is not valid.

Heat flow values of 30-40 m W/m^2 are typical of many subduction complexes (Anderson et al., 1976; Pavlis and Bruhn, 1983). This observation is also in accord with measurements taken north of Cape Mendocino, where heat flow ranges from 34 to 55 m W/m^2 and averages 43 m W/m^2 (Lachenbruch and Sass, 1980). The thermal conductivities of sediments in submarine accretionary prisms are relatively low; estimates for the Aleutian trench slope, for examples, are approximately 2.4 mcal/cm-s-^oC (McCarthy et al. 1984), so the geothermal gradient for the Aleutian slope is 20.8 -22.7^oC/km (McCarthy et al., 1984). If the subduction-accretion models for northern California are basically correct (e.g., Bachman, 1982), then these Aleutian data help constrain the choice of geothermal gradient for the Franciscan Complex. In conclusion, we believe a value of 23^oC/km is geologically reasonable for the purpose of calculating first approximations of maximum burial depths within the study area.

RESULTS

Central Belt

Twenty-nine samples collected from the Franciscan Central belt were measured for vitrinite reflectance (Strong, 1986) (Appendix B). Mean reflectance (Rm) ranges from 0.68% to 1.41%, and the average Rm is 0.98% (Fig. 4). According to the Price model, these values correspond to a temperature range of 137^oC to 233^oC and an average temperature of 185^oC (Fig. 5). Depths of burial were approximately 5600 meters to 9900 meters, assuming a surface temperature of 10^oC and a geothermal gradient of 23^oC/km.

The most prominent trend in thermal maturity for the Central belt is an eastward increase in reflectance values (Fig. 6). Iso-reflectance contouring highlights this progression, and contour lines are at least subparallel to the fault contact with the Yager complex. If the documented levels of thermal maturation are a consequence of structural and/or stratigraphic burial (and not shear heating), then this pattern signifies an increase in burial depth toward the east; evidently, uplift combined with subsequent erosion has exposed progressively deeper levels of the melange belt from west to east.

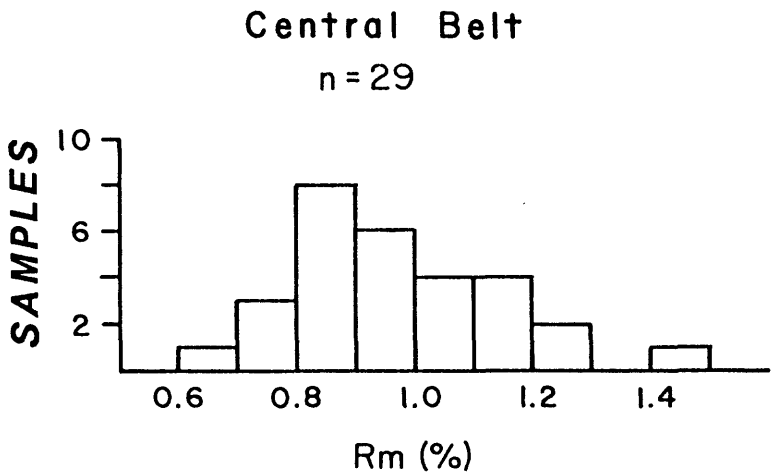

FIGURE 4. Histogram showing the range of mean Ro values for twenty-nine samples obtained from the Franciscan Central belt. Data for each individual sample are listed in Appendix B.

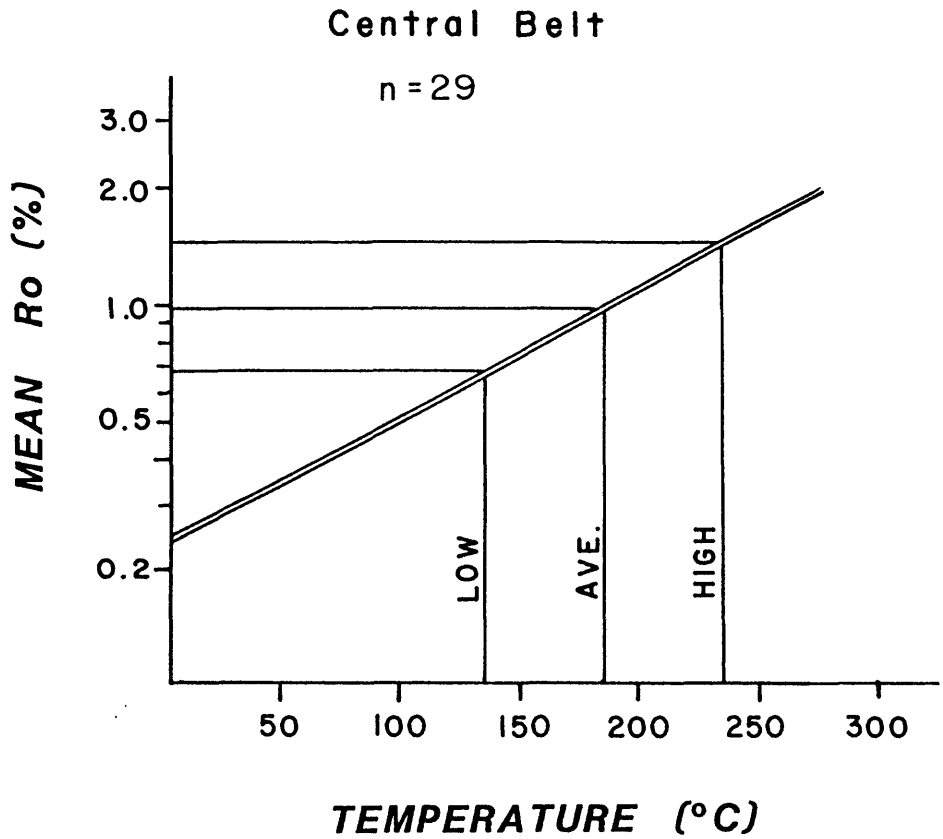

FIGURE 5. Values of mean vitrinite reflectance and corresponding estimates of peak paleotemperature for the Franciscan Central belt. The correlation between Rm and temperature is from Price (1983). See Appendix B for complete list of data.

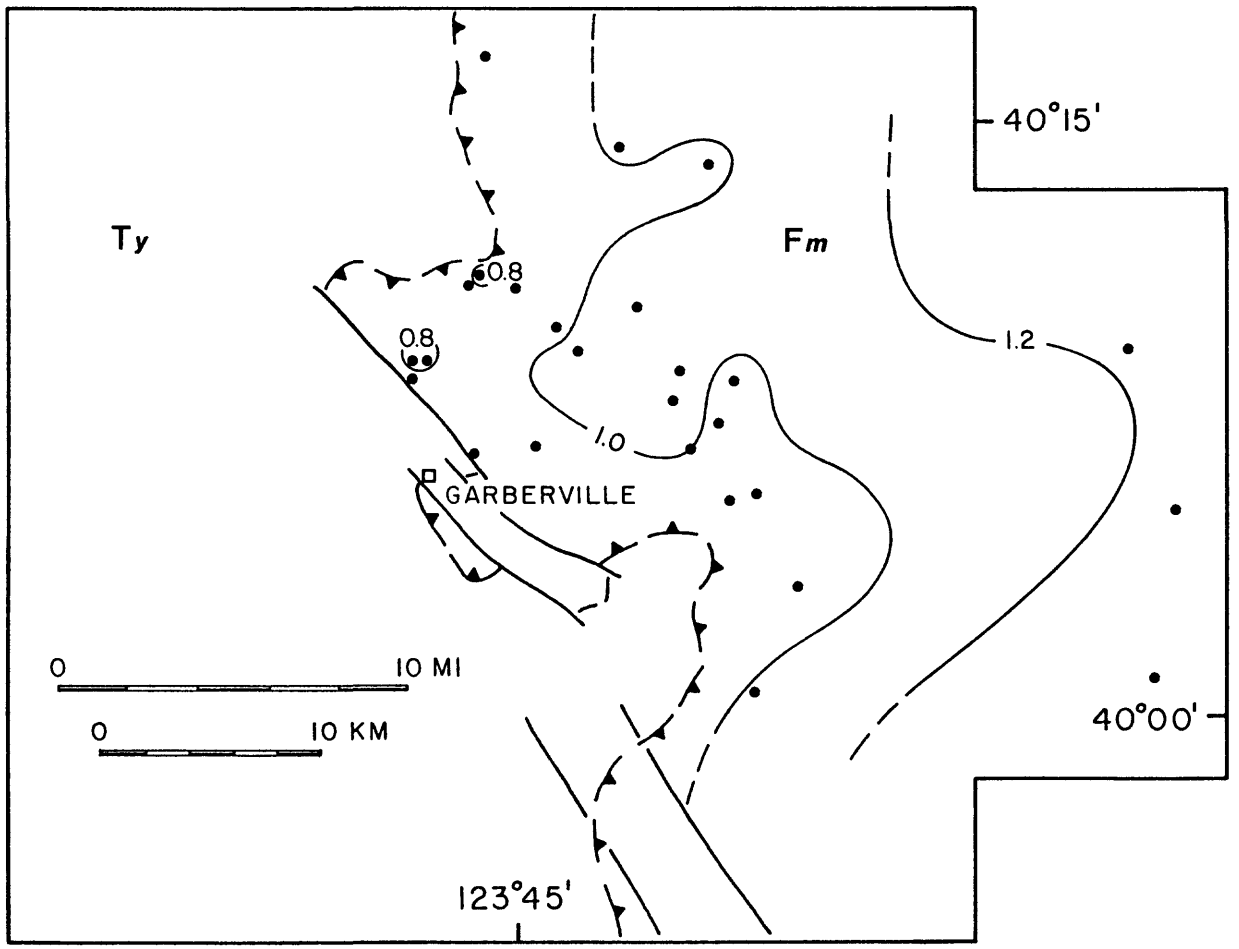

FIGURE 6. Contour map of mean vitrinite reflectance for the Franciscan Central belt (Fm). Thrust symbol depicts the Eel River fault, which separates Central belt melange from the Yager complex (Ty). Solid dots indicate control points. The obvious eastward increase in Rm can be attributed to greater uplift and unroofing of the melange in that direction.

The vitrinite data correspond well to other data on paleotemperature conditions in the Central belt. The characteristic metamorphic mineral of the Central belt is pumpellyite, with or without lawsonite (Blake et al., 1967), and these minerals are stable within the temperature range indicated by Rm data (Turner, 1981). X-ray analyses indicate that the melange matrix was subjected to temperatures of between 100° and 250°C and pressures between 3 and 10 kb, and the high phengitic content of micas suggests that much of the Central belt was buried to depths of 15 to 20 km (Cloos, 1983). These data seemingly require geothermal gradients substantially lower than our chosen regional average of 23°C/km, perhaps on the order of 10-15°C/km. Suppressed gradients of this magnitude, however, may be typical of many accretionary wedges (Pavlis and Bruhn, 1983; Cloos, 1985).

Yager Complex

Thirty-eight samples from the Yager complex yielded Rm values (Strong, 1986) (Appendix B). In addition, twenty-five previous analyses from within the study area (Underwood, 1985) are included in our evaluation for a total of 63. Mean reflectance ranges from 0.40% to 1.08%, and the average mean reflectance is 0.68% (Fig. 7). The minimum and maximum peak burial temperatures are 67° and 189°C respectively, and the average peak temperature is 137°C (Fig. 8). These data compare favorably with those of Underwood and O'Leary (1985) whose study area lies immediately south of the region described here (Fig. 1).

As in the Central belt, the iso-reflectance contours roughly parallel the Yager structural grain (Fig. 9). There is an eastward increase in Rm in the southern half of the study area, and this increase has been attributed to progressive tectonic burial of Yager strata beneath the Eel River fault (Underwood, 1985). Data from farther north, however, demonstrate that the overall pattern of thermal maturity is more complicated. The pattern near Weott consists of two thermal highs flanking a central low (Fig. 9), and this mimics the trend expected with a large syncline. We believe the Weott region is best explained by broad synformal warping of the Yager section during late Cenozoic time. Folds in the Neogene Wildcat Group, which unconformably overlies the Yager complex, probably are cogenetic, and the Eel River fault was broadly warped during the same tectonic event. It may be that the monoclinal gradient near Garberville represents one flank of a major Quaternary fold.

If the levels of thermal maturity are simply related to depth of Yager burial (stratigraphic and/or structural), then the minimum and maximum depths were approximately 2500 meters and 8300 meters, respectively, and the average depth was 5600 meters. As discussed subsequently, the highest reflectance values were obtained near Bridgeville and Redway, and these values are probably the result of shear heating along the Eel River fault. It would be misleading to use these data to estimate the maximum burial depth, so a more realistic maximum burial depth is 7000 meters based on an Rm of 0.86% and a corresponding temperature estimate of 167°C.

Coastal Belt

Thirty-one samples collected from the Franciscan Coastal belt contain sufficient vitrinite for reflectance measurements (Strong, 1986) (Appendix B). Mean reflectance ranges from 0.47% to 1.78%, and the average Rm is 0.77% (Fig. 10). The corresponding paleotemperatures are 88°C and 260°C, with an average of 153°C (Fig. 11). This average may be misleading, however, because a histogram plot of all Coastal belt data indicates that three values are substantially higher (Fig. 10). Furthermore, all three of these samples were

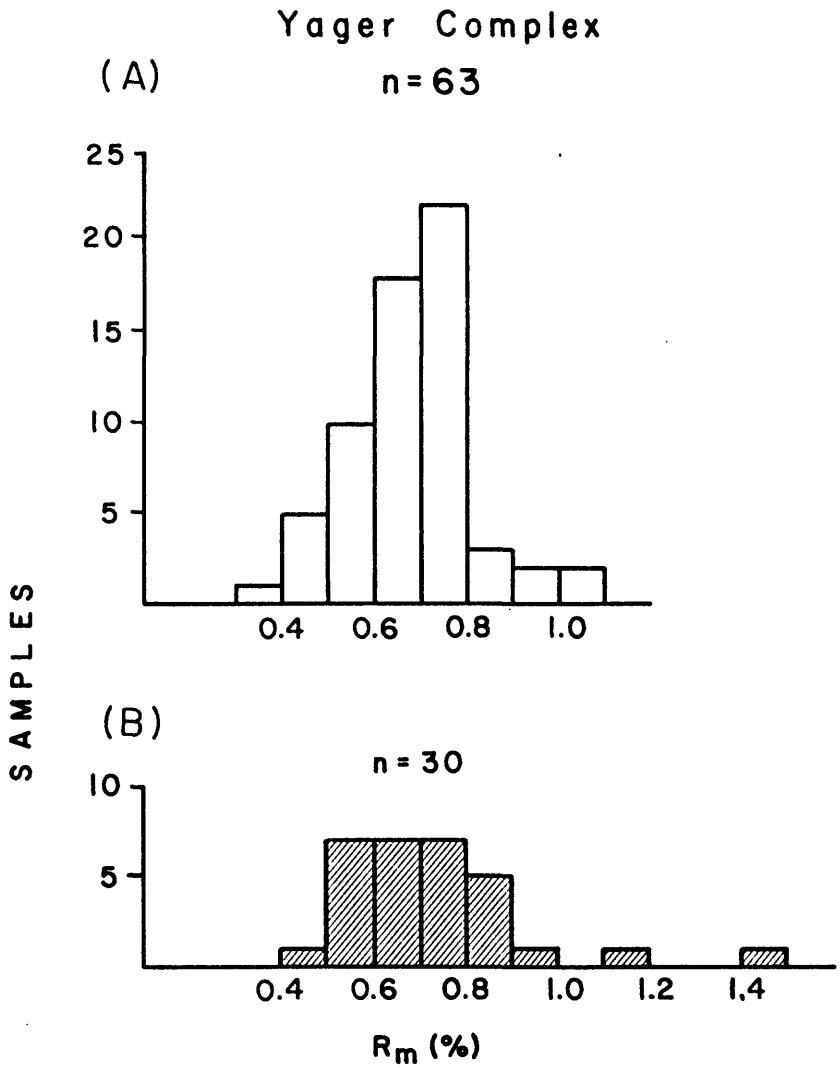

FIGURE 7. Histograms showing the range of mean Ro values for all samples collected from the Yager complex. Diagram A includes values for the study area outlined in Figure 2. Diagram B shows data from analogous Yager strata located farther south in Mendocino County (Fig. 1)(Underwood and O'Leary, 1985). See Appendix B for complete listing of data. Twenty-five samples from the northern study area are discussed further in Underwood (1985).

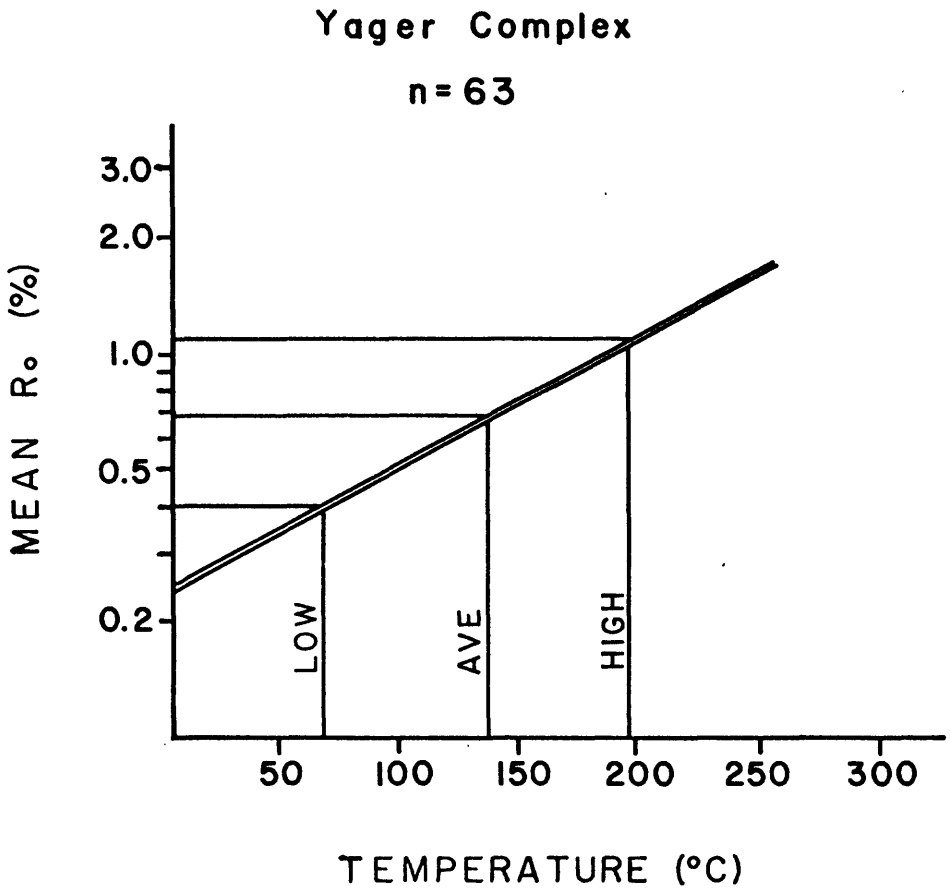

FIGURE 8. Values of mean vitrinite reflectance and corresponding estimates of peak paleotemperature for the northern portion of the Yager complex. Correlation between Rm and temperature is from Price (1983). See Underwood (1985) and Appendix B for complete listings of data.

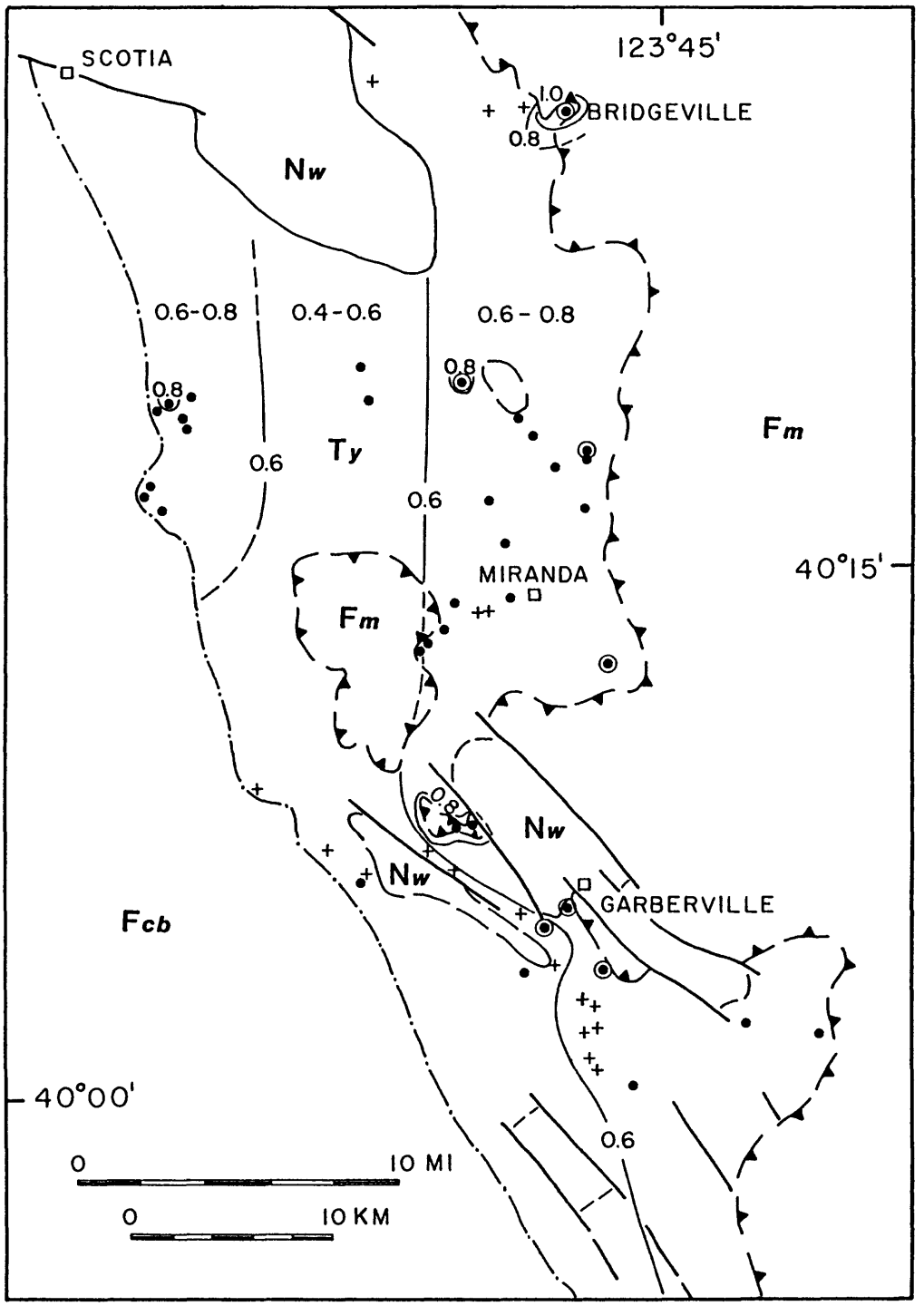

FIGURE 9. Contour map of mean vitrinite reflectance for the northern portion of the Yager complex (Ty). Other rock units include the Franciscan Central belt (Fm), the Franciscan Coastal belt (Fcb), and the Wildcat Group (Nw). Solid dots and crosses represent control points; crosses indicate localities discussed by Underwood (1985).

collected near the border of the King Range terrane, which apparently has undergone a widespread thermal overprint (see next section for discussion of King Range-Point Delgada data). If the three high values are removed from the main population, the range of the mean reflectance changes to 0.47% to 0.95%, with an average mean reflectance of 0.71%. The modified temperature average is thus 142°C (Fig. 11).

There are few obvious spatial trends in thermal maturity within the Coastal belt in our study area. The highest values border the King Range, and there is a broad region of low maturity immediately east of Point Delgada (Fig. 12). When comparisons are made with Mendocino County to the south (Underwood and O'Leary, 1985), there is a slight northward increase in reflectance values (Fig. 10). This increase could be related to the aforementioned thermal overprint in the King Range-Point Delgada area. Alternatively, perhaps the rate or magnitude of uplift increased slightly to the north, but this is difficult to substantiate with existing data.

By attributing thermal maturity to burial overburden alone, the required burial depths range from 3400 meters to 7400 meters (excluding samples bordering the King Range). The average burial depth is 5700 meters. All of these calculations are based upon the assumptions of a 10°C surface temperature and a thermal gradient of 23°C/km.

King Range-Point Delgada

Eleven samples from the King Range and three from Point Delgada yielded vitrinite reflectance measurements (Strong, 1986). The minimum mean reflectance is 0.77% the maximum is 2.50%, and the average Rm is 1.65% (Fig. 13). It should be noted that all three Point Delgada samples were high: 2.15%, 2.17%, 2.50%. The minimum and maximum values correspond to a temperature range of 153°C to 308°C, and the average peak temperature was 252°C (Fig. 14).

The well-defined thermal aureole centered at Point Delgada affects rocks of both King Range and Coastal belt affinity (Fig. 12). Mean reflectance diminishes gradually in all directions, and the overprint definitely crosses the terrane boundary mapped by McLaughlin and others (1982) to affect Coastal belt rocks. The documented pattern of thermal maturation cannot be a consequence of structural and/or stratigraphic burial, because the overburden would have to increase by several kilometers in a roughly concentric pattern over a distance of only five kilometers. Such a scenario is geologically unreasonable. Instead, the region probably was affected by post-accretionary hydrothermal activity; studies of sulfide vein mineralization at Point Delgada (McLaughlin et al., 1985) provide strong supporting evidence for this hypothesis. Fluid-inclusion data indicate that vein homogenization temperatures were as high as 287°C. This temperature agrees favorably with our data from Point Delgada which indicate an average temperature of 295°C. K-Ar dating of adularia shows that the timing of mineralization was 13.8 $\pm$ 0.4 Ma (McLaughlin et al., 1985).

An event involving high heat flow during middle or late Miocene time is problematic. One possible source of heat would be a so-called slab window associated with the northward-migrating Mendocino triple junction and San Andreas fault (Dickinson and Snyder, 1979; Furlong, 1984). However, according to conventional plate reconstructions (e.g., Atwater and Molnar, 1973), this scenario would require deposition and accretion of King Range strata well south of their present location, with subsequent northward translation of perhaps 400 km (McLaughlin et al., 1985). An alternative and less mobilistic

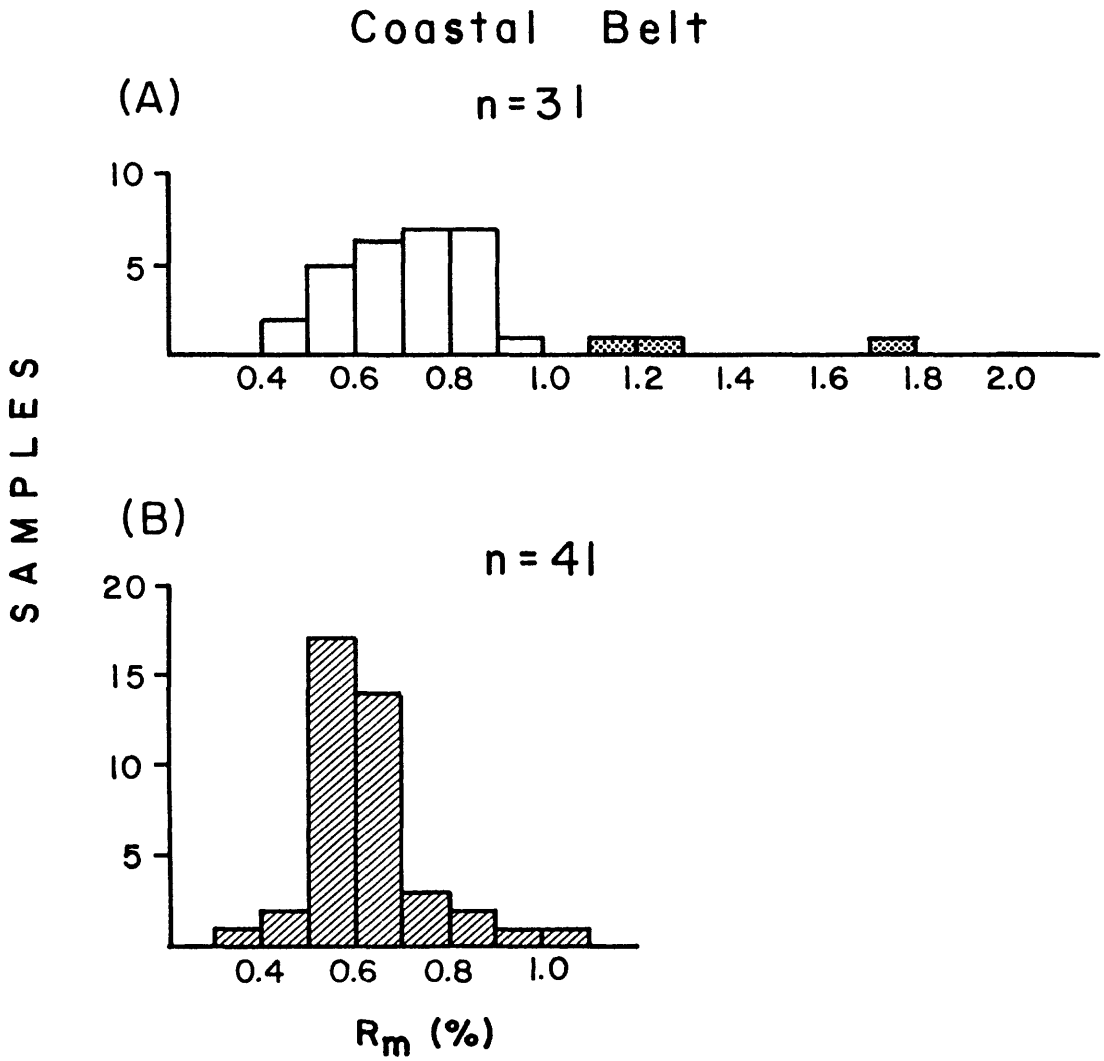

FIGURE 10. Histograms showing the range in mean Ro values for the Franciscan Coastal belt. Diagram A includes data for rocks within the study area outlined in Figure 2; the three samples with unusually high Rm values were obtained near the boundary of the King Range terrane. Diagram B shows data from Mendocino County to the south (Fig. 1) (Underwood and O'Leary, 1985). See Appendix B for a complete listing of data from Humboldt County.

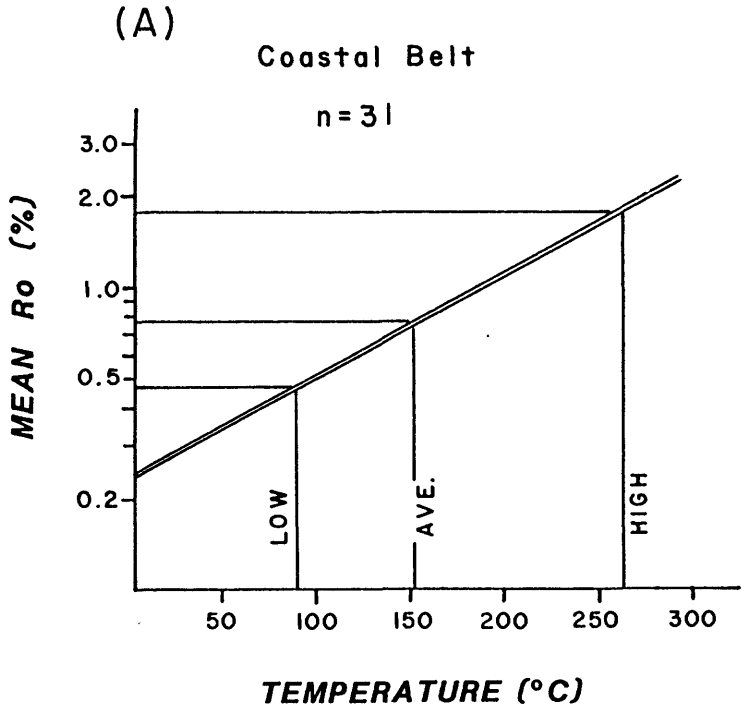

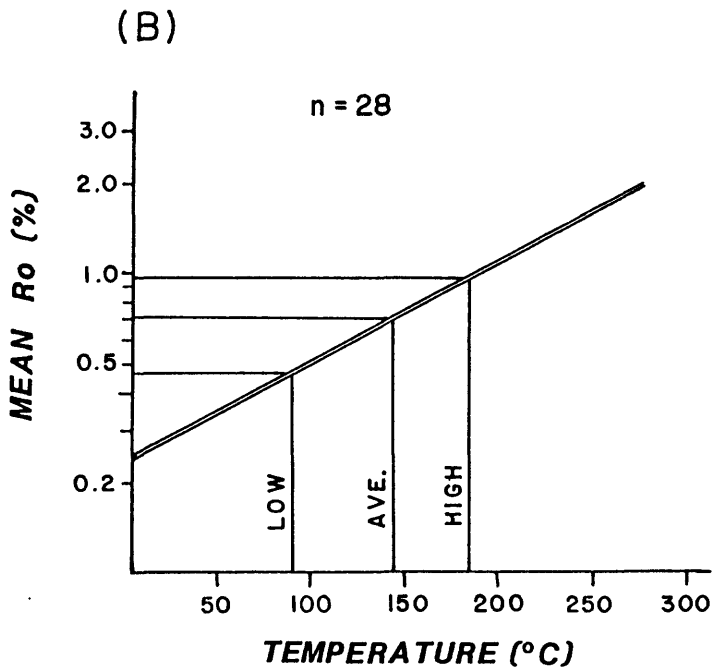

FIGURE 11. Values of mean vitrinite reflectance and corresponding estimates of paleotemperature for the Franciscan Coastal belt of Humboldt County. Diagram A includes all samples collected within the study area; diagram B deletes the three high values associated with the King Range boundary. Correlation between Rm and peak temperature is from Price (1983).

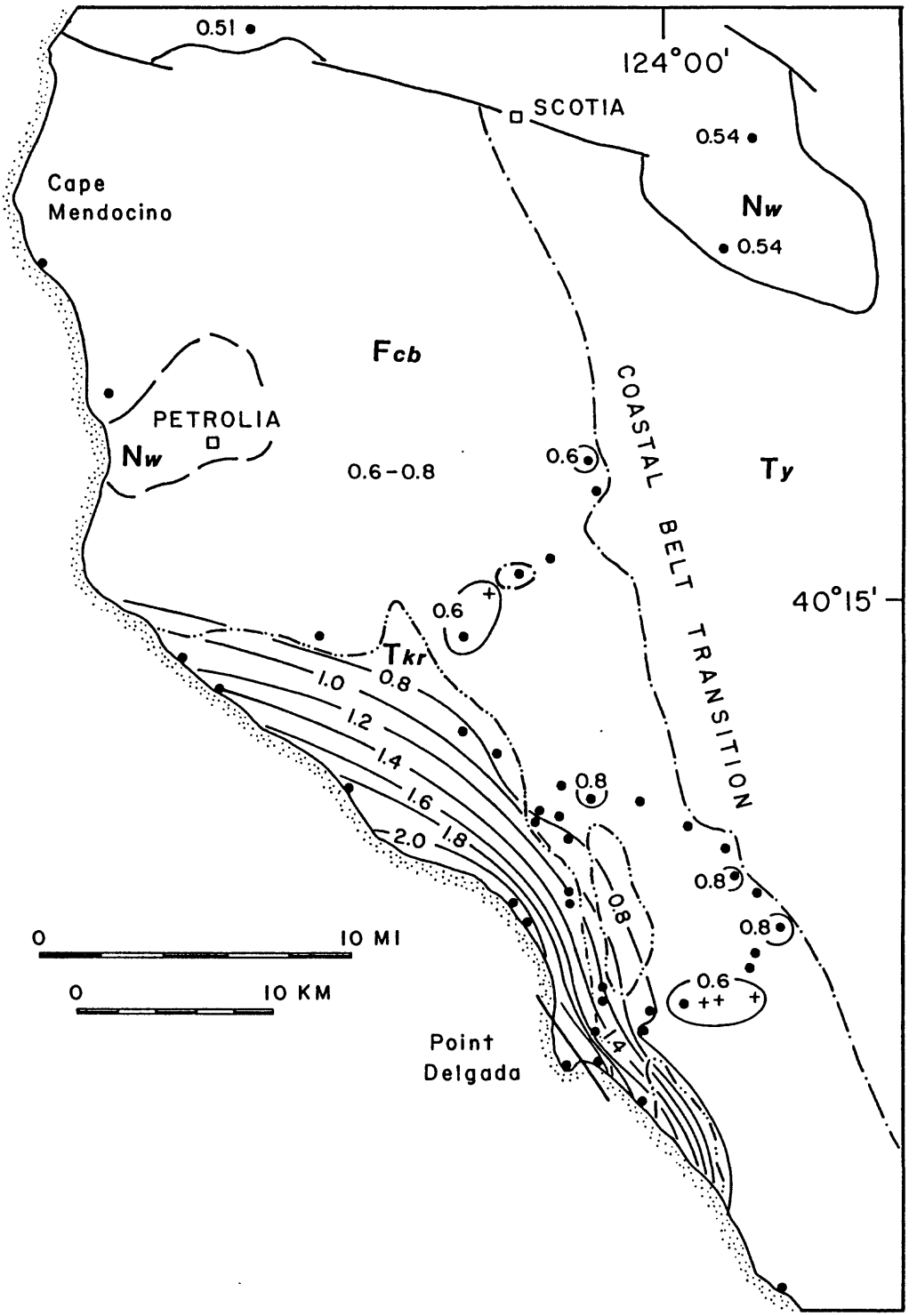

FIGURE 12. Contour map of mean vitrinite reflectance for the Franciscan Coastal belt (Fcb) and the King Range terrane (Tkr). Additional rock units include the Yager complex (Ty) and the Wildcat Group (Nw). Solid dots and crosses indicate control points, with crosses representing data from O'Leary et al (1984).

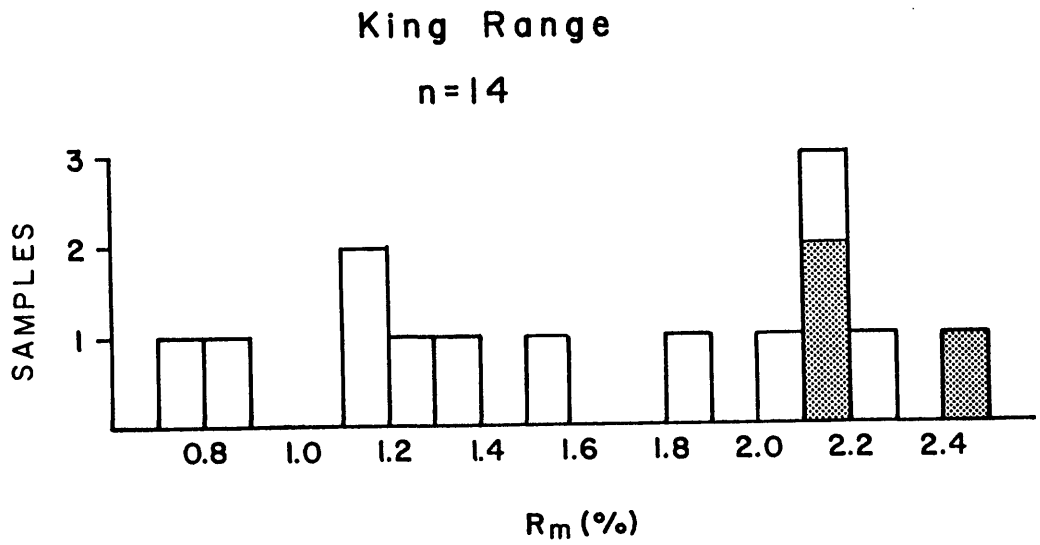

FIGURE 13. Histogram showing range in mean Ro values for the King Range and Point Delgada (stippled). Data for each of the fourteen individual samples are listed in Appendix B.

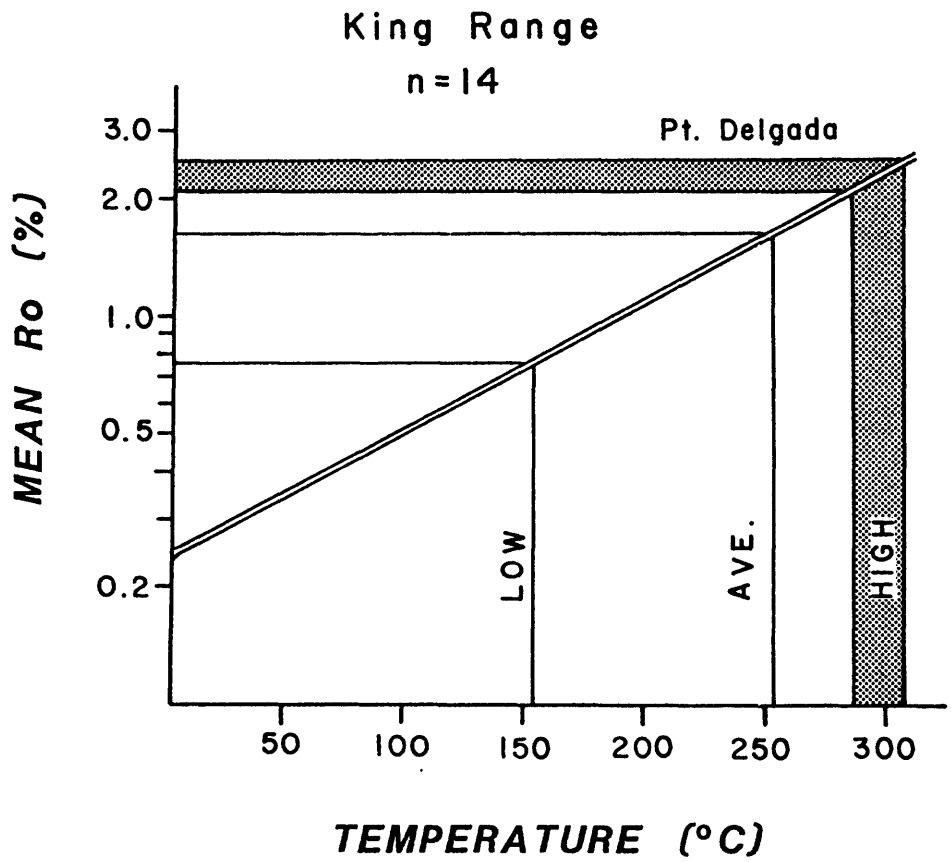

FIGURE 14. Values of mean vitrinite reflectance and corresponding estimates of peak paleotemperature for the King Range terrane. Stippled pattern depicts data from Point Delgada. Correlation between Rm and temperature is from Price (1983). See Appendix B for complete listing of data.

hypothesis places the anomalous heat source in the subducting Farallon plate, perhaps due to off-ridge volcanism, fracture-zone instability, or the close proximity of the Farallon-Pacific ridge to the Franciscan subduction front. Whatever the source, the hydrothermal overprint affected both King Range and Coastal belt strata shortly after the terranes were sutured together.

Wildcat Group

Vitrinite reflectance measurements were made on only three samples from the Wildcat Group (Appendix B). The values are 0.54, 0.54, and 0.51%, with an average mean reflectance of 0.53% (Fig. 12). Paleotemperatures are in the range of 99° to 106°C, and the average temperature was 104°C. Because only three data points of similar value are available, iso-reflectance contouring is not possible. However, these values are important for establishing the post-Miocene geothermal gradient within the Eel River basin. Structural data (Ogle, 1953) demonstrate that stratigraphic overburden above the sampling sites is roughly 2000 m (equivalent to the section measured at Centerville Beach; Ingle, 1976). The geothermal gradient, therefore, was probably as high as 45°C/km during Wildcat deposition.

Present-day heat flow in the vicinity of Scotia (Fig. 1) has been measured at 1.31 HFU (55 mW/m^2) (Lachenbruch and Sass, 1980). This level of heat flow, combined with a geothermal gradient of 45°C/km, would require a thermal conductivity of approximately 2.9 mcal/cm-s-°C; this conductivity value is well within the range expected for poorly indurated marine sediments such as those of the Wildcat Group. Moreover, a substantial rise in regional geothermal gradient during the Neogene (compared to our estimates of 23°C/km for Paleogene strata) is consistent with the dramatic hydrothermal event centered at Point Delgada at approximately 13 Ma (McLaughlin et al., 1985).

Eel River Fault

Samples from two locations indicate that shear heating has occurred along the Eel River fault. At Bridgeville (Fig. 15), the footwall was heated to temperatures as high as 197°C (Rm = 1.08%, Sample M80-51; data from Underwood, 1985). Roughly two kilometers to the west, temperatures in the Yager dropped to around 140°C (Rm = 0.72%, Underwood, 1985). West of Redway (Fig. 15), peak temperatures in the Yager footwall were elevated to approximately 182°C adjacent to the fault (Samples EV 15-21,22) but cooled to background values of around 96°-118°C within one kilometer of the fault (Underwood, 1985).

The paleotemperature estimates cited above are minimum values based upon the equilibration rates documented by Barker (1983) and Price (1983). It is probable, however, the short-term temperatures within the fault zone were significantly higher. For example, Bostick (1973) produced mean reflectance values of around 1.0% by heating coals in the laboratory for one hour at about 350°. The thermal aureoles associated with the Eel River fault are discussed in greater detail by Underwood (1985) and Underwood and Strong (in review).

Regional Summary

Table I and Figures 16 and 17 summarize the vitrinite-reflectance and paleotemperature data from our study. Regional gradients in thermal maturity are complicated by temporal variations in tectonic process, geothermal gradient, and hydrothermal activity. Within Central belt melange east of the Eel River fault, there is a clear increase in Rm from west to east (Fig. 17). Coastal belt strata west of Garberville are more mature than adjacent Yager strata; this type of pattern is consistent with the trench-slope depositional

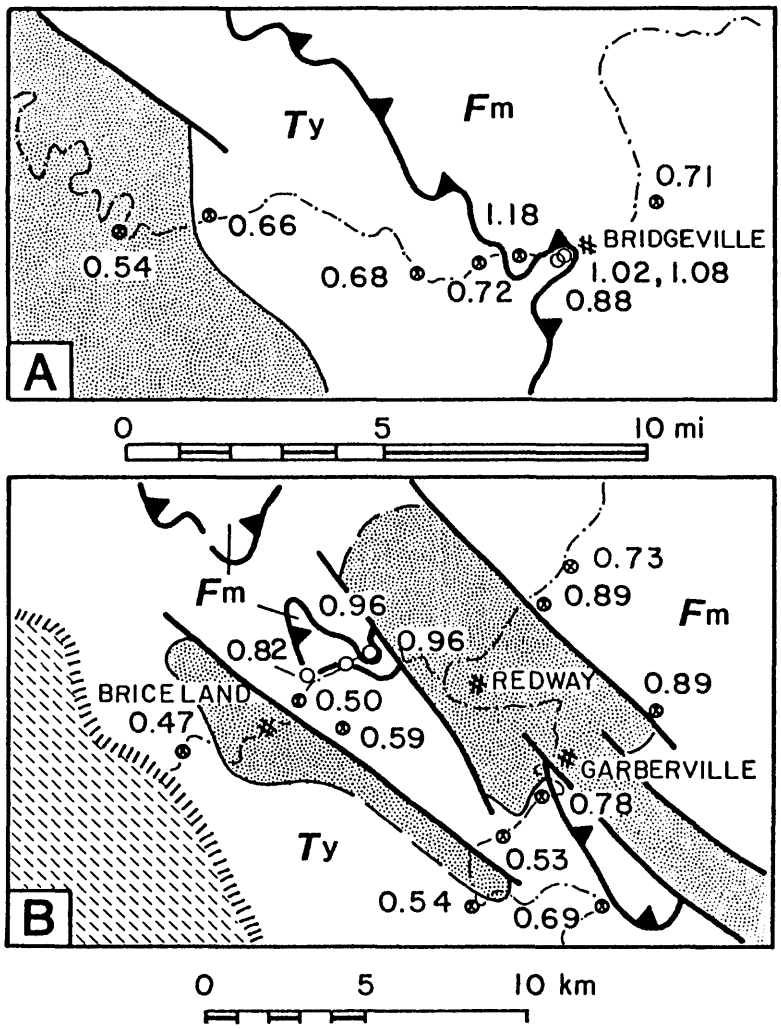

FIGURE 15. Examples of probable shear-heating anomalies associated with the Eel River fault. In example A (Bridgeville locality), Rm values for Yager shales in the footwall are as high as 1.08%; maximum values away from the thrust contact are only 0.72%. In example B (Redway locality), Yager values near the fault trace range from 0.82% to 0.96%Rm; background levels of thermal maturity are only 0.59% to 0.50%Rm. The significance and cause of these anomalies are discussed in greater detail by Underwood and Strong (in review).

model proposed for the Yager complex (e.g., Underwood, 1985). However, Yager strata west of Miranda display maturities equal to or greater than the inferred Coastal belt basement. Consequently, the geometry, displacement history, and tectonic significance of the Coastal belt transition remains open to question. The hydrothermal anomaly centered at Point Delgada extends across the entire King Range and overprints some coastal belt rocks; the ultimate heat source for this anomaly is uncertain, but high heat flow persisted through Neogene time and also affected deposits of the Wildcat Group. Finally, spatial trends at the present-day erosional surface have been modified by late Cenozoic megascopic folds, high-angle faults, and differential uplift.

TABLE 1. SUMMARY OF DATA

		MEAN Ro (%)			PALEOTEMP (°C)*		
TERRANE	No.	High	Low	Ave	High	Low	Ave
Central	29	1.41	0.68	0.98	233	137	185
Yager	63	1.08	0.40	0.68	197	67	137
Coastal	31	1.78	0.47	0.77	260	88	153
Coastal**	28	0.95	0.47	0.71	181	88	142
King R.	11	2.21	0.77	1.48	290	153	237
Pt. Del.	3	2.50	2.15	2.27	308	288	295
Wildcat	3	0.54	0.51	0.53	106	99	104

*Based upon Rm-Temp correlation of Price (1983)

**Excluding sample sites bordering King Range

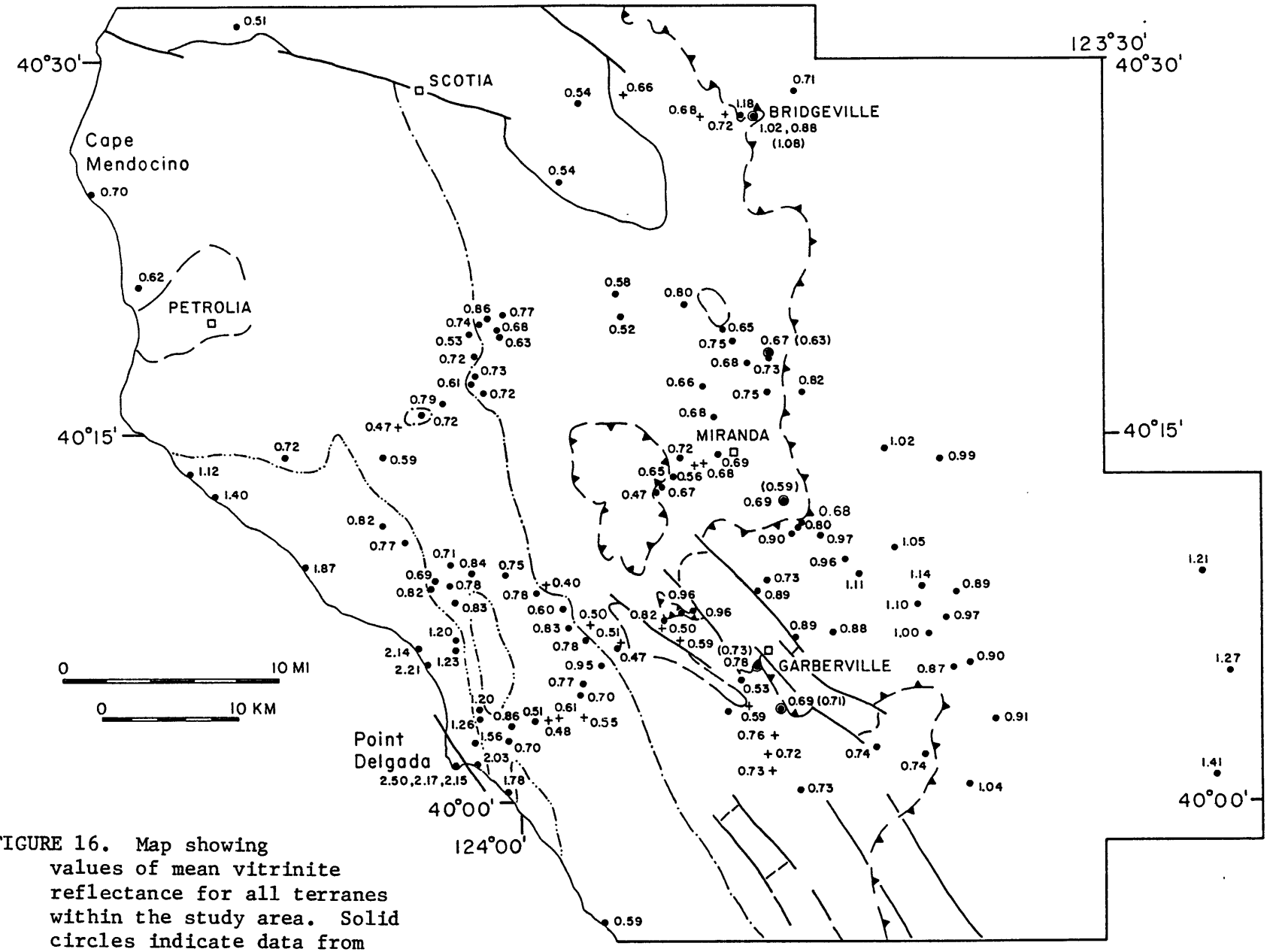

FIGURE 16. Map showing values of mean vitrinite reflectance for all terranes within the study area. Solid circles indicate data from Strong (1986).

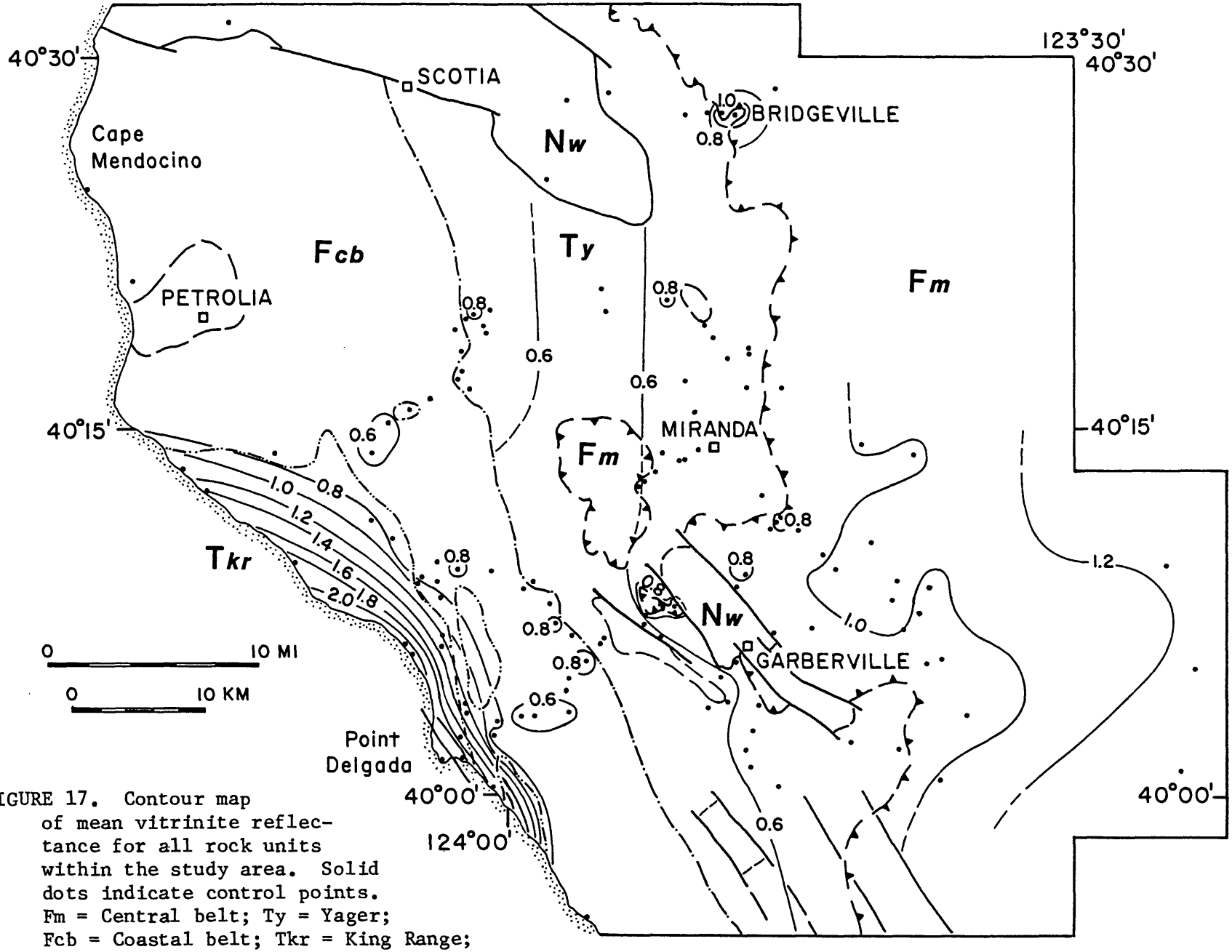

FIGURE 17. Contour map of mean vitrinite reflectance for all rock units within the study area. Solid dots indicate control points. Fm = Central belt; Ty = Yager; Fcb = Coastal belt; Tkr = King Range; Nw = Wildcat Group.

APPENDIX A. TECHNIQUES OF SAMPLE SELECTION, PREPARATION, MEASUREMENT, AND STATISTICAL EVALUATION

Sample Selection

As mentioned in the Introduction, there are several problems inherent in the technique of vitrinite reflectance. The first is related to alteration of vitrinite particles by weathering and oxidation at or near the surface. Surface weathering can produce multimodal patterns on histograms depicting random reflectance (Marchioni, 1983), and the weathering effect can extend as far as 10 meters below the surface. In order to minimize this effect, pains were taken to select the freshest possible samples from outcrops. Fresh shales are common within drainage channels and beachcliff exposures, but it was more difficult to find fresh occurrences of scaly argillites which typify the Coastal belt and Central belt.

Direct comparisons between water-washed samples and roadcut samples show no systematic variation in mean reflectance. Moreover, because most weathered grains display oxidation halos, cracks, pits, or other morphologic anomalies, they are easily eliminated from the data population. Consequently, we believe the use of surface samples has had minimal influence on the results of our study. It should also be noted that actual measurements made from oxidation halos yielded lower reflectance values than similar measurements made on unaltered cores.

Kerogen Concentration

Measurements of organic-carbon content demonstrate that most Franciscan shales from northern California are depleted in organic matter, with typical values ranging between 0.35 and 0.65 wt-% carbon (Underwood, 1985; unpublished data). Consequently, organic matter had to be extracted and concentrated before measurements of vitrinite reflectance could be completed. Even with these concentrations, some samples proved to be virtually barren of vitrinite. The laboratory methods used are as follows:

Approximately 10 to 20 grams of sample were processed. Each sample was rinsed under distilled water, scrubbed with a stiff brush, and then dried prior to crushing. Samples were crushed in an iron mortar to fragments roughly 3 mm in size. The fragments were then placed in 1000 ml polyethylene beakers and allowed to soak overnight in 100 ml of 10% hydrochloric acid to remove any carbonates. The acid was poured off, and 100 ml of distilled water added to the sample.

Silicates were removed by adding 100-200 ml of 52% hydrofluoric acid. Because of the harmful effects associated with this acid, all work with the HF was done under a fume hood using full protective gear (face shield, rubber gloves, apron, etc.). Furthermore, the reaction of HF with silicate minerals can generate considerable heat, even to the point of violent boiling. Such heat may be sufficient to affect the thermal maturity of low-rank kerogens (100^{o} = 0.51% Ro). To control the reaction, the acid was added slowly in 25 ml increments, and distilled water was added after each increment. Each sample is then placed on a magnetic stirrer and agitated for at least an hour. The sample remains in the HF for several hours to ensure that all silicates are removed.

Following removal of the silicates, the acid and acid residues were rinsed from the samples. Either of two rinsing procedures was followed:

1.) Immediately after the HF treatment is complete, the sample is decanted into two 50 ml polyethylene centrifuge tubes. This material is centrifuged until the kerogen settles to the bottom of the tube; the clear liquid is then poured off into a plastic waste container for disposal. This step is repeated until all of the sample is decanted. Then the sample is rinsed with distilled water and centrifuged, again discarding the residual liquid. This water rinsing is repeated at least four times.

2.) Alternatively, when the HF treatment is complete, the beaker is filled to the brim with distilled water. The sample is allowed to settle for several hours, or overnight. The clear liquid is then poured off into a plastic storage bottle, with care not to pour away any of the kerogen. The remaining sample is then rinsed and centrifuged, as in method 1.

The kerogen in the bottom of the centrifuge tubes was then scraped into an aluminum dish and dried under a low temperature heat lamp. Finally, the dried kerogen clumps were ground to a fine powder in a mortar and stored in plastic vials.

Slide Preparation

Slides of the kerogen concentrate were prepared in the following manner. A small amount of "Hillquist" slow-curing epoxy (C-D components) is mixed with the powdered kerogen concentrate in an aluminum dish. Enough kerogen extract is added so that the kerogen/epoxy mixture becomes very viscous but retains a smooth texture (not "gritty"). Too much kerogen in the epoxy causes difficulties in obtaining a smooth polished surface. This mixture is allowed to set for 15 minutes.

While the epoxy is setting, one side of a petrographic slide can be frosted (using a coarse grit) and thoroughly dried to ensure that the epoxy will adhere to the slide. With the polishing equipment described below, drops of epoxy on the corners of slides are not necessary.

Following the drying of the slide, a two centimeter diameter pellet of the partially-set kerogen/epoxy mixture is applied to the center of the frosted slide. The slide is cured for an additional 30 minutes at room temperature on a perfectly horizontal surface. The finished slide is then placed on a warming tray and cured at between 30 to 40 degrees Celsius for an additional 24 hours. Curing slides at temperatures higher than these may cause slides to crack during polishing because the epoxy has cured too rapidly. Conceivably, higher temperatures could also modify the reflectance.

Slide Polishing

The first step in polishing the slides is to cut a flat, even surface on the epoxy pellet. We found this step was best accomplished using a thin-section grinding wheel, slowly and evenly grinding the pellet down to a thickness of 1 mm. The resulting surface was then polished on a standard lap using a Buehler "Petrothin" attachment and Buehler "Texmet" lap cloths. The "Petrothin" attachment is an automatic device which holds three slides flat against the polishing lap and rotates them as the lap spins. The succession of grit sizes used is as follows: 3-micron diamond paste for approximately 10 to 15 minutes, 0.3-micron alumina slurry for 10 minutes, 0.05-micron alumina slurry for 10 minutes. The slides must be cleaned between each step using an ultrasonic cleaner and soap, and then dried before moving to the next size

grit. At the end of the polishing sequence, the epoxy pellet should have a uniform glassy surface, and the organic matter should have very few scratches when viewed at high magnification. The slides must be stored in a dessicator for at least 1 hour prior to observation in order to remove any remaining moisture. This drying step is important because moisture content can affect Ro values (Suggate and Lowrey, 1982).

Data Collection

Observations in reflected light were made using a 50x oil-immersion lens and a 16x ocular mounted on a Leitz Ortholux research microscope set up in the reflected light mode. A Keithly 244 high-voltage power supply and a Hewlett-Packard direct-current power supply provided stable power to the photometer and the light source, respectively. Reflected light was directed to a Leitz MPV-1 photometer through a 70-micron diameter diaphragm (constricted to a 4-micron opening during calibration), and the Ro value was read on a Keithly 177 Microvolt digital voltmeter. Calibration of the photometer for a linear response was performed weekly using a polished reflectance standard. All five values (0.299, 0.506, 0.940, 1.025, 1.672) were measured during these checks. In addition, two values on the standard were always measured before any specific session. Given the range of our data, these values were typically the 0.506% and 0.940% squares. If the mean Ro of a measured slide was above that range, the next appropriately higher Ro square on the standard was rechecked to insure correct linearity.

The criteria used to choose particles to measure are described in Dow and O'Connor (1982). The first step is obviously to distinguish vitrinite from other types or organic matter. In coal petrography, distinguishing the different types of organic macerals is straightforward. However, dispersed organic particles can be small, fragmented, and sparsely distributed on the slide. In our study, vitrinite particles were recognized on the basis of morphology, color, and texture of the polished surface.

Any particles that have rounded edges were eliminated from the data because the likelihood of recycling. In addition, particles that display numerous pits or cracks were regarded as weathered or oxidized and eliminated from the data. Thus, the only measurements incorporated into our data set were derived from particles of sufficient size and appropriate morphology. About 50 data points must be gathered from each sample to assure statistically valid results.

Above reflectance values of about 1.5%, convergence begins to occur between the reflectivity of vitrinite and other organic macerals (Bostick, 1979; Tissot and Welte, 1984) and proper selection becomes increasingly dependent upon morphologic criteria. At lower levels of maturation, it is a common practice to identify vitrinite on the basis of relative reflectivity or a "lowest gray" scale. Such methods require abundant kerogen, however, so that direct comparisons of macerals can be made within a single field of view. In order to avoid bias toward a "correct" reflectance value in lean samples we depended strongly on morphologic criteria to select vitrinite particles (see Stach, 1975).

Data Reduction and Interpretation

Individual vitrinite particles are generally anisotropic in their reflectance, with the degree of anisotropy increasing at higher levels of thermal maturity (Stach, 1975). The dispersed organic matter from Franciscan shales

was randomly oriented in epoxy plugs, so the problem of anisotropy was overcome by counting approximately 50 grains and calculating a mean value. Past studies have demonstrated that this technique is statistically sound and useful in practice (Dow and O'Conner, 1982; Houseknecht and Matthews, 1985). In addition, the relatively low levels of maturation displayed by most samples from our study are not associated with strong degrees of anisotropy.

Vitrinite particles are fairly resistant to weathering, and grains can be recycled from older sedimentary strata. Reflectance values are sensitive only to the peak heating event in the overall sedimentary history of a vitrinite particle, so recycled grains can be reset in accordance with a subsequent higher-temperature burial event. However, particles can also be recycled from sedimentary sequences that are more thermally mature than the present host rock. Under such circumstances, failure to recognize recycled grains will lead to mean reflectance values that are erroneously high.

In order to help identify recycled vitrinite, it is common practice to plot reflectance data in histogram form (Dow and O'Conner, 1982). The shape of a histogram will be strongly dependent on the chosen sampling interval, but in most cases a Gaussian distribution of Ro values is evident and calculations of mean and standard deviation are completed using all available data points. In other cases, a population of vitrinite is distinctly bimodal or multimodal. By convention, the lowest mode is assumed to represent the true thermal maturity of the indigenous population. Modes with higher values are labeled "reworked" and eliminated from calculations of mean reflectance.

If a clear bimodal trend is evident, or a few isolated values are much higher than the majority, it is a straightforward decision to eliminate "recycled" grains. However, samples which display complicated multimodal patterns inhibit objective identification of a recycled population (Fig. 3). Multimodal distributions can be caused by surface weathering (Marchioni, 1983), and turbiditic shales are commonly bimodal or multimodal (Castano and Sparks, 1974). Moreover, the inference of recycling should be consistent with independent geologic information linking the depositional environment to a suitable source terrane with elevated thermal maturity. In the case of the Franciscan Complex, such a link is difficult to establish (e.g., Dickinson et al., 1979; Nilsen and McKee, 1979).

In conclusion, subjective or unspecified criteria for removal of allegedly recycled vitrinite can introduce bias into the data and lower the degree of reproducibility. According to our established convention, higher Ro values are eliminated from calculations of mean reflectance only if there is a gap of at least 0.10% Ro (one sampling interval).

Accuracy

Our results have been compared directly to measurements made at two independent commercial laboratories to test for accuracy. Each of the other laboratories also measured thermal alteration index (TAI) as a check on their values of mean Ro. The results of these comparisons are shown in Appendix C. In general, values from the UMC lab are within 0.10% Rm of the other measurements. It is important to note that the two commercial labs also differ among themselves by about the same magnitude. Some of the slightly higher, values may be a consequence of our conservative convention for elimination of recycled gains. In light of these findings, we believe variations in reflectance of more than 0.15% Rm are geologically significant.

APPENDIX B. TABULATION OF VITRINITE REFLECTANCE DATA

Key

Location - given in coordinates of township, range, section.

n = number of measurements in data population associated with a particular sample

R = range in random reflectance readings for a particular sample

S = standard deviation

X = arithmetic mean

Temp = estimated paleotemperature in ^{o}C, based upon the correlation between vitrinite reflectance and temperature established by Price (1983)

SAMPLE NUMBER	TERRANE	LOCATION	VITRINITE REFLECTANCE				TEMP (°C)
			n	R	S	X	
M83-101	Yager	T5S R3E S1	30	0.36-1.05	0.18	0.69	139
M83-102	Yager	T4S R3E S26	29	0.27-0.80	0.13	0.53	104
M83-103	Yager	T4S R3E S25	50	0.42-1.18	0.21	0.78	155
M83-104	Yager	T3S R3E S13	50	0.41-1.05	0.17	0.69	139
M83-106	Yager	T2S R3E S28	44	0.65-1.20	0.15	0.88	171
M83-107	Coastal belt	T4S R2E S28	50	0.48-1.11	0.18	0.77	153
M83-112	Point Delgada	T5S R1E S16	36	2.11-2.92	0.22	2.50	308
M83-113	Point Delgada	T5S R1E S16	45	1.70-2.77	0.29	2.17	289
M83-114	Point Delgada	T5S R1E S16	45	1.72-2.60	0.23	2.15	288
M83-115	Coastal belt	T5S R1E S2	48	0.84-1.77	0.25	1.26	218
M83-116	Coastal belt	T5S R1E S3	40	0.90-1.44	0.14	1.20	211
M83-119	King Range	T4S R1E S21	48	0.86-1.71	0.23	1.23	215
M83-122	King Range	T4S R1E S21	41	0.84-1.48	0.17	1.20	211
M83-124	Coastal belt	T5S R1E S12	49	0.52-1.06	0.13	0.70	140
M83-126	Yager	T4S R2E S23	45	0.30-0.79	0.11	0.47	88
M83-127	Coastal belt	T4S R2E S15	45	0.39-1.16	0.19	0.78	155
M83-128	Coastal belt	T4S R2E S16	40	0.56-1.06	0.12	0.83	163
M83-129	Coastal belt	T4S R2E S8	49	0.31-0.90	0.16	0.60	120
M83-130	Coastal belt	T4S R2E S6	85	0.43-1.21	0.20	0.78	155
M83-131	Coastal belt	T3S R1E	64	0.42-1.29	0.21	0.82	161
M83-132	Coastal belt	T3S R1E	58	0.50-1.25	0.20	0.85	166
M83-134	Coastal belt	T3S R1E	77	0.40-0.98	0.14	0.69	139
M83-136	Coastal belt	T4S R1E S4	128	0.38-1.51	0.29	0.82	161
M83-137	Coastal belt	T4S R1E S9	105	0.44-1.40	0.23	0.83	163
M83-139	Coastal belt	T4S R1E S5	76	0.40-1.00	0.13	0.67	135
M83-140	Coastal belt	T4S R1E S5	63	0.40-1.20	0.19	0.82	161
M83-143	King Range	T3S R1E	40	0.40-1.19	0.23	0.77	153
M83-145	King Range	T3S R1W	41	0.50-1.10	0.19	0.82	161
M83-146	Coastal belt	T3S R1W S1	29	0.18-1.09	0.26	0.59	118
M83-149	Yager	T3S R3E S7	49	0.39-0.99	0.18	0.65	131
M83-150	Yager	T3S R3E S7	45	0.38-0.99	0.16	0.67	135
M83-151	Yager	T3S R3E S13	40	0.37-0.66	0.07	0.47	88
M83-153	Yager	T3S R3E S5	50	0.35-1.01	0.16	0.72	144
M83-156	Yager	T3S R3E S4	50	0.40-1.10	0.18	0.69	139
M83-157	Yager	T1S R2E S35	50	0.31-0.88	0.14	0.52	101

SAMPLE NUMBER	TERRANE	LOCATION	VITRINIITE REFLECTANCE				TEMP (°C)
			n	R	S	X	
M83-158	Yager	T1S R2E S27	42	0.41-0.80	0.09	0.58	116
M83-159	Yager	T1S R3E S32	43	0.49-1.05	0.15	0.80	158
M83-161	Yager	T2S R3E S4	50	0.41-0.94	0.15	0.65	131
M83-162	Yager	T2S R3E S3	30	0.57-1.16	0.13	0.75	149
M83-164	Yager	T2S R3E S12	30	0.32-1.02	0.17	0.67	135
M83-165	Yager	T2S R3E S12	45	0.44-1.08	0.15	0.73	146
M83-166	Yager	T2S R3E S14	50	0.43-1.04	0.14	0.68	137
M83-169	Central belt	T2S R4E S19	47	0.49-1.15	0.19	0.82	161
M83-170	Yager	T2S R3E S24	50	0.57-0.98	0.10	0.75	149
M83-172	Yager	T2S R3E S21	50	0.49-0.89	0.11	0.66	133
M83-173	Yager	T2S R1E	30	0.35-1.03	0.20	0.63	127
M83-174	Yager	T2S R1E	50	0.39-1.12	0.20	0.68	137
M83-175	Yager	T1S R1E S35	49	0.47-1.04	0.16	0.77	153
M83-176	Yager	T2S R1E	40	0.61=1.35	0.19	0.86	167
M83-177	Yager	T2S R1E	42	0.47-1.22	0.21	0.74	148
M83-178	Coastal belt	T2S R1E	48	0.32-0.74	0.10	0.53	104
M83-179	Coastal belt	T2S R1E	40	0.40-1.04	0.16	0.72	144
M83-180	Yager	T2S R1E S22	40	0.43-1.13	0.17	0.73	146
M83-181	Yager	T2S R1E S22	49	0.35-0.91	0.13	0.53	104
M83-183	Coastal belt	T2S R1E S28	63	0.30-1.45	0.23	0.79	156
M83-184	Coastal belt	T2S R1E S31	50	0.41-1.13	0.20	0.72	144
M83-186	Yager	T2S R1E S22	50	0.34-1.21	0.18	0.72	144
M83-187	Wildcat	T1N R2E S32	50	0.35-0.88	0.14	0.54	106
M83-190	Central belt	T1N R3E S15	47	0.74-1.48	0.17	1.18	209
M83-191	Yager	T1N R3E S14	64	0.61-1.23	0.16	0.87	169
M83-192	Yager	T1N R3E S14	50	0.61-1.51	0.21	1.02	190
M83-193	Central belt	T1N R4E S7	47	0.43-1.04	0.17	0.71	142
M83-194	Wildcat	T1N R2E S16	44	0.27-0.88	0.17	0.54	106
M83-195	Wildcat	T2N R2W S26	49	0.30-0.82	0.12	0.51	99
M83-196	Coastal belt	T1S R3W S3	50	0.50-0.94	0.14	0.70	140
M83-199	Coastal belt	T1S R3W S25	50	0.45-0.86	0.09	0.62	124
EV15-21	Yager	T4S R3E S8	48	0.64-1.28	0.16	0.96	182
EV15-22	Yager	T4S R3E S8	46	0.65-1.33	0.17	0.96	182
EV15-24	Central belt	T4S R3E S1	39	0.63-1.11	0.14	0.89	172
EV15-26	Central belt	T3S R3E S36	50	0.46-1.11	0.15	0.73	146

SAMPLE NUMBER	TERRANE	LOCATION	VITRINIITE REFLECTANCE				TEMP (°C)
			n	R	S	X	
EV15-28	Central belt	T3S R4E S30	47	0.42-1.00	0.17	0.68	137
EV15-29	Central belt	T3S R4E S19	49	0.55-1.35	0.21	0.90	173
EV15-30	Central belt	T3S R4E S19	50	0.47-1.18	0.20	0.80	158
EV16-1	Central belt	T4S R5E S8	50	0.56-1.37	0.22	0.97	183
EV16-6	Central belt	T4S R5E S4	49	0.49-1.25	0.22	0.89	172
EV16-15	Central belt	T3S R4E S25	40	0.75-1.28	0.13	1.05	194
EV16-18	Central belt	T3S R4E S34	49	0.71-1.40	0.19	1.11	201
EV16-22	Central belt	T3S R4E S34	49	0.65-1.30	0.16	0.96	182
EV16-30A	Central belt	T4S R5E S6	50	0.90-1.47	0.15	1.14	205
EV16-32A	Central belt	T4S R5E S6	45	0.81-1.34	0.14	1.10	200
EV16-35	Central belt	T3S R5E S5	48	0.70-1.24	0.13	0.99	186
EV16-38	Central belt	T3S R4E S2	50	0.70-1.28	0.17	1.02	190
EV16-41	Central belt	T3S R4E S29	40	0.72-1.29	0.16	0.97	183
EV19-1B	King Range	T5S R1E S10	55	1.27-1.91	0.19	1.56	246
EV19-9	Coastal belt	T5S R1E S1	50	0.59-1.31	0.17	0.86	167
EV20-4	Coastal belt	T5S R2E S6	50	0.40-0.67	0.06	0.51	99
EV20-8	Coastal belt	T4S R2E S33	45	0.42-1.14	0.22	0.70	140
EV20-10	Coastal belt	T4S R2E S22	49	0.59-1.39	0.19	0.95	181
EV20-14A	Yager	T4S R3E S18	60	0.55-1.20	0.18	0.82	161
EV21-11	Yager	T5S R3E S3	58	0.36-0.72	0.09	0.54	106
EV21-21	Yager	T5S R4E S20	47	0.49-1.13	0.14	0.73	146
EV21-28	Central belt	T4S R4E S17	47	0.55-1.18	0.17	0.89	172
EV22-4	Yager	T5S R5E S7	50	0.43-1.06	0.14	0.74	148
EV22-5	Central belt	T4S R4E S15	47	0.60-1.20	0.16	0.88	171
EV22-9	Central belt	T4S R5E S18	47	0.75-1.34	0.16	1.00	187
EV22-12	Central belt	T4S R5E S28	48	0.53-1.14	0.16	0.87	169
EV22-19	Yager	T5S R4E S11	50	0.41-1.04	0.15	0.74	148
EV23-6	Central belt	T5S R5E S21	47	0.72-1.39	0.18	1.04	192
EV23-14C	Central belt	T5S R5E S2	49	0.57-1.27	0.18	0.91	175
EV23-17	Central belt	T4S R5E S21	50	0.60-1.31	0.19	0.90	173
84-ZJ-4	Central belt	T3S R7E S32	50	0.89-1.65	0.17	1.21	212
84-LMJ-1	Central belt	T5S R7E S21	50	1.09-1.85	0.18	1.41	232
84-LMJ-3	Central belt	T4S R7E S33	60	0.92-1.55	0.17	1.27	219
84-LRJ-2b	Central belt	T5S R7E S15	48	0.93-1.55	0.15	1.19	210
MK-44	Coastal belt	T3S R1W S7	50	0.51-1.05	0.11	0.72	144

SAMPLE NUMBER	TERRANE	LOCATION	VITRINIITE REFLECTANCE				
			n	R	S	X	TEMP (^{o}C)
MK-50	King Range	T3S R2W S9	60	0.74-1.53	0.22	1.12	202
MK-55	King Range	T3S R2W S15	50	0.98-1.91	0.23	1.40	232
MK-57	King Range	T4S R1E S18	50	1.71-2.54	0.20	2.14	287
MK-58	King Range	T3S R1W S32	85	1.36-2.43	0.27	1.87	270
MK-78	King Range	T5S R1E S15	50	1.60-2.47	0.27	2.03	280
MK-94	King Range	T4S R1E S20	55	1.83-2.59	0.21	2.21	292
MK-102	Coastal belt	T5S R1E	50	1.35-2.25	0.25	1.78	263
M80-86	Coastal belt	T5S R2E	64	---	0.17	0.54	106
M80-88	Coastal belt	T5S R2E	50	---	0.18	0.48	91
M81-29	Coastal belt	T2S R1W 536	48	---	0.14	0.47	88

APPENDIX C. COMPARISON OF VITRINITE REFLECTANCE VALUES*

Sample Number	GeoChem** LABS	Clark*** Geological Services	University of Missouri
1	0.68	0.59	0.60
2	0.73	0.64	0.66
3		0.47	0.46
4	0.66	0.59	0.53
5		1.31	1.45
6		0.51	0.61/0.59
7	0.63	0.64	0.67/0.67
8		0.53	0.63
9	1.08		1.02
10	0.59		0.69
11	0.71		0.69
12	0.73		0.78
13	0.51		0.47
14			0.63/0.63

*Multiple runs either performed on the same sample or multiple samples collected from the same outcrop.

**GeoChem Laboratories, Inc., Houston, Texas

***Clark Geological Services, Fremont, California

REFERENCES CITED

Ammosov, I. I., Babashkin, B. G., and Sharkova, L. S., 1975, Bituminite of Lower Cambrian deposits in the Irkutsk oil and gas region, in I. V. Yeremin ed., Paleotemperatury zon nefteobrazovaniya: Moscow, Nauka Press, p. 25-59.

Anderson, R. N., Uyeda, S., and Miyashiro, A., 1976, Geophysical and geochemical constraints at converging plate boundaries, I, Dehydration in the downgoing slab: Geophysical Journal of the Royal Astronomical Society, v. 44, p. 333-357.

Atwater, T., and Molnar, P., 1973, Relative motion of the Pacific and North American plates deduced from sea-floor spreading in the Atlantic, Indian, and South Pacific Oceans, in Proceedings of the conference on tectonic problems of the San Andreas Fault system: Stanford University Publications Geological Sciences, v. 13, p. 136-148.

Bachman, S. B., 1978, A Cretaceous and early Tertiary subduction complex, Mendocino Coast, northern California, in Howell, D. G. and McDougall, K. A., eds., Mesozoic paleogeography of the western United States: Society of Economic Paleontologist and Mineralogists and Pacific Section, Pacific Coast Paleogeography Symposium 2, p. 419-430.

Bachman, S. B., 1982, The Coastal Belt of the Franciscan: youngest phase of northern California subduction, in Leggett, J. K., ed., Trench-forearc geology: Sedimentation and tectonics on modern and ancient active plate margins: Geological Society of London Special Publication 10, p. 401-417.

Bachman, S. B., Underwood, M. B., and Menack, J. S., 1984, Cenozoic evolution of coastal northern California, in J. K. Crouch and S. B. Bauchman, eds., Tectonics and sedimentation along the California margin: Society of Economic Paleontologists and Mineralogists Pacific Section, v. 38, p. 55-66.

Barker, C. E., 1983, Influence of time on metamorphism of sedimentary organic matter in liquid dominated geothermal systems, western North America: Geology, v. 11, p. 384-388.

Beutner, E. C., and McLaughlin, R. J., Ohlin, H. N., and Sorg, D. H., 1980, Geologic map of the King Range and Chemise Mountain instant study areas of northern California: U. S. Geological Survey Miscellaneous Field Studies Map 1196A, scale 1:62,500.

Blake, M. C., Irwin, W. P., and Coleman, R. G., 1967, Upside-down metamorphic zonation, blueschist facies, along a regional thrust in California and Oregon: U. S. Geological Survey, Professional Paper, 575-C: p. 1-9.

Blake, M. C., Jr., and Jones, D. L., 1974, Origin of Franciscan melanges in northern California, in Dott, R. H., and Shaver, R. H., eds., Modern and ancient geosynclinal sedimentation: Society of Economic Paleontologist and Mineralogists Special Publication 19, p. 345-357.

Blake, M. C., Jr., and Jones, D. L., 1981, The Franciscan assemblage and related rocks in northern California: a reinterpretation, in Ernst, W. G., ed., The Geotectonic Development of California: Englewood Cliffs, N. J., Prentice-Hall, Inc., p. 307-328.

Bostick, N. H., 1973, Time as a factor in thermal metamorphism of phytoclasts (coaly particles): Cong. Internat. Strat. Geol. Carbonif., 7th, Krefeld, Compte Rendu, v. 2, p. 183-193.

Bostick, N. H., 1974, Phytoclasts as indicators of thermal metamorphism, Franciscan Assemblage and Great Valley Sequence (Upper Mesozoic), California: Geological Society of America Special Paper 153, p. 1-17.

Bostick, N. H., 1979, Microscopic measurement of the level of catagenesis of solid organic matter in sedimentary rocks to aid exploration for petroleum and to determine former burial temperatures - A review, in Scholle, P. A., and Schluger, P. R., eds., Aspects of diagenesis: Society of Economic Paleontologist and Mineralogists Special Publication 26, p. 17-43.

Bostick, N. H., and Cashman, S. M., McCulloh, T. M., and Waddell, C. T., 1978, Gradients of vitrinite reflectance and present temperature in the Los Angeles and Ventura Basins, California, in D. F. Oltz, ed., Low temperature metamorphism of kerogen and clay minerals: Society of Economic Paleontologist and Mineralogists Pacific Section, p. 65-96.

Castano, J. R., and Sparks, D. M., 1974, Interpretation of vitrinite reflectance measurements in sedimentary rocks and determination of burial history using vitrinite reflectance and authigenic minerals: Geological Society of America Special Paper 153, p. 31-52.

Cloos, M., 1983, Comparative study of melange matrix and metashales from the Franciscan subduction complex with the basal Great Valley Sequence, California: Journal of Geology, v. 91, p. 291-306.

Cloos, M., 1984, Landward-dipping reflectors in accretionary wedges: active dewatering conduits?: Geology, v. 12, p. 519-522.

Cloos, M., 1985, Thermal evolution of convergent plate margins: thermal modeling and reevaluation of isotopic Ar-ages for blueschists in the Franciscan Complex of California: Tectonics, v. 4, p. 421-434.

Dickinson, W. R., and Snyder, W. S., 1979, Geometry of triple junctions related to San Andreas transform: Journal of Geophysical Research, v. 84, p. 561-572.

Dickinson, W. R., Ingersoll, R. V., and Grahman, S. A., 1979, Paleogene sediment dispersal and paleotectonics in northern California: summary: Geological Society of America Bulletin, Part II, v. 90, p. 1458-1528.

Dow, W. G., 1977, Kerogen studies and geological interpretations: Journal of Geochemical Exploration, v. 7, p. 79-99.

Dow, W. G., and O'Connor, D. I., 1982, Kerogen maturity and type by reflected light mircoscopy applied to petroleum generation, in How to assess maturation and paleotemperatures: Society of Economic Paleontologists and Mineralogists Short Course 7, p. 133-157.

Ernst, W. G., 1971, Do mineral paragenesis reflect unusually high-pressure conditions of Franciscan metamorphism?: American Journal of Science, v. 270, p. 81-108.

Ernst, W. G., 1983, Phanerozoic continental accretion and the metamorphic evolution of northern and central California: Tectonophysics, v. 100, p. 287-320.

Ernst, W. G., 1984, California blueschists, subduction, and the significance of tectonostratigraphic terranes: Geology, v. 12, p. 436-440.

Ernst, W. G., Seki, Y., Onuki, H., and Gilbert, M. C., 1970, Comparative study of low-grade metamorphism in the California Coast Ranges and the Outer Metamorphic Belt of Japan: Geological Society of America Memoir 124, 276 p.

Evitt, W. R., and Pierce, S. T., 1975, Early Teritary ages from the Coastal Belt of the Franciscan Complex, northern California: Geology, v. 3, p. 433-436.

Furlong, K.P., 1984, Lithospheric behavior with triple junction migration: an example based on the Mendocino triple junction: Physics of the Earth and Planetary Interiors, v. 36, p. 213-223.

Ghent, E. D., 1979, Problems in zeolite facies geothermometry, geobarometry, and fluid compositions: Society of Economic Paleontologist and Mineralogists Special Publication 26, p. 81-87.

Herd, D. G., 1978, Intracontinental plate boundary east of Cape Mendocino, California: Geology, v. 6, p. 721-725.

Hood, A. Gutjahr, C. C. M., and Heacock, R. L., 1975, Organic metamorphism and the generation of petroleum: American Association Petroleum Geologist Bulletin, v. 59, p. 986-996.

Houseknecht, D. W., and Matthews, S. M., 1985, Thermal maturity of Carboniferous strata, Ouachita Mountains: American Association Petroleum Geologist Bulletin, v. 69, p. 335-345.

Hutton, A. C., and Cook, A. C., 1980, Influence of alginite on the reflectance of vitrinite from Joadja, New South Wales, and some other coals and oil shales containing alginite: Fuel, v. 59, p. 711-714.

Jones, D. L., Blake, M. C., Jr., Bailey, E. H., and McLaughlin, R. J., 1978, Distribution and character of Upper Mesozoic subduction complexes along the west coast of North America: Tectonophysics, v. 47, p. 207-222.

Lachenbruch, A. H., and Sass, J. H., 1980, Heat flow and energetics of the San Andreas fault zone: Journal of Geophysical Research, v. 85, p. 6185-6222.

Marchioni, D. L., 1983, The detection of weathering in coal by petrographic, rheologic, and chemical methods: International Journal of Coal Geology, v. 2, p. 231-259.

McCarthy, J., Stevenson, A. J., Scholl, D. W., and Vallier, T. L., 1984, Speculations on the petroleum geology of the accretionary body: an example from the central Aleutians: Marine and Petroleum Geology, v. 1, p. 151-167.

McLaughlin, R. J., Kling, S. A., Poore, R. Z., McDougall, K., and Beutner, E. C., 1982, Post-middle Miocene accretion of Franciscan rocks, northwestern California: Geological Society of America, v. 93, p. 595-605.

McLaughlin, R. J., Sorg, D. H., Morton, J. L., Theodore, R. G., and Meyer, C. E., 1985, Paragenesis and tectonic significance of base and precious

metal occurrences along the San Andreas Fault at Point Delgada, California: Economic Geology, v. 80, p. 344-359.

Newman, J., and Newman, N. A., 1982, Reflectance anomalies in Pike River coals: evidence of variability in vitrinite type, with implications for maturation studies and "Suggate rank": New Zealand Journal of Geology and Geophysics, v. 25, p. 233-243.

Nilsen, T. H., and McKee, E. H., 1979, Paleogene paleogeography of the western United States, in Armentrout, J. M., et al., eds., Cenozoic paleogeography of the western United States: Society of Economic Paleontologist and Mineralogists, Pacific Section, Pacific Coast Paleogeography Symposium 3, p. 257-276.

Ogle, B. A., 1953, Geology of Eel River Valley area, Humboldt County, California: California Division of Mines and Geology Bulletin 164, 128 p.

Pavlis, T. L., and Bruhn, R. L., 1983, Deep-seated flow as a mechanism for the uplift of broad forearc ridges and its role in the exposure of high P/T metamorphic terranes: Tectonics, v. 2, p. 473-497.

Price, L. C., 1983, Geologic time as a parameter in organic metamorphism and vitrinite reflectance as an absolute paleogeothermometer: Journal of Petroleum Geology, v. 6, p. 5-38.

Price, L. C., and Barker, C. E., 1985, suppression of vitrinite reflectance in amorphous rich kerogen-a major unrecognized problem: Journal of Petroleum Geology, v. 8., p. 59-84

Stach, E., 1975, Stack's textbook of coal petrology: Gebruder, Borntraeger, 428 p.

Strong, R. H., 1986, Thermal maturity of Franciscan and related strata, southern Humboldt County, northern California (unpubl. M.S. thesis): University of Missouri, Columbia, 160 p.

Suggate, R. P., 1982, Low-rank sequences and scales of organic metamorphism: Journal of Petroleum Geology, v. 4, p. 377-392.

Suggate, R. P., and Lowrey, J. H., 1982, The influence of moisture content on vitrinite reflectance and the assessment of maturation of coal: New Zealand Journal of Geology and Geophysics, v. 25, p. 227-231.

Tissot, B. P., and Welte, D. H., 1984, Petroleum formation and occurrence (second edition): New York, Springer-Verlag, 699 p.

Turner, F., 1981, Metamorphic Petrology (second edition): McGraw Hill, 524 p.

Underwood, M. B., 1982, The Garberville thrust - a contact of probable Miocene age within the Franciscan Complex, northern California: Geological Society of America Abstracts with Programs, v. 14, p. 635-636.

Underwood, M. B., 1983, Depositional setting of the Paleogene Yager formation, northern Coast Ranges of California, in D. Larue and R. Steel, eds., Cenozoic marine sedimentation, Pacific margin, U.S.A.: Society of Economic Paleontologist and Mineralogists, Pacific Section, p. 81-101.

Underwood, M. B., 1984, Franciscan and related rocks of southern Humboldt County, northern California Coast Ranges: analysis of structure, tecton-

ics, sedimentary petrology, paleogeography, depositional history, and thermal maturity (unpubl. Ph.D. dissertation): Cornell University, 354 p.

Underwood, M. B., 1985, Sedimentology and hydrocarbon potential of the Yager Structural complex, possible Paleogene source rocks in the Eel River basin, northern California: American Association Petroleum Geologist Bulletin 69, p. 1088-1100.

Underwood, M. B., and O'Leary, J. D., 1985, Vitrinite reflectance and paleotemperature within Franciscan terrantes of coastal northern California: 738°45'N to 40°00'N: U.S. Geological Survey Open-File Report 85-663, 32 p.

Waples, D. W., 1980, Time and temperature in petroleum formation: application of Lopatin's method to petroleum exploration: American Association Petroleum Geologist Bulletin, v. 64, p. 916-926.

Wright, N. J. R., 1980, Time, temperature, and organic maturation - the evolution of rank within a sedimentary pile: Journal of Petroleum Geology, v. 2, p. 411-425.